Available online at www.garmian.edu.krd

Passer Journal of Basic and Applied Sciences

Passer 8 (Issue 1) (2026) 545-564

Original Article

Numerical Study on the Mechanisms of Heat Transfer in Packed and Fluidized Configurations

Sherko Ahmad Flamarz Al-Arkawazi * [1]

[1] *Electrical & Computer Engineering Department, Kalar Technical College, Garmian Polytechnic University (GPU), Kalar 46021, Al Sulaymaniyah, Kurdistan Reign, Iraq.*

Received 05 January 2026; revised 28 February 2026;
accepted 15 March 2026; available online 24 March 2026

DOI: 10.24271/PSR.2026.570929.2498

ABSTRACT

A numerical study was carried out to assess the contribution of the primary heat transfer mechanisms in packed and fluidized beds using a CFD-DEM thermal model. This study aims to compare the contribution of conduction, convection, and radiation heat transfer under the same operating conditions, and investigate the impact of particle material, size, inlet fluid velocity (0.08-0.16 m/s), and at a constant wall temperature over the range (100 -500 ºC). Aluminium and chromium oxide particles were used to examine the impact of thermo-physical properties on the thermal performance of the bed. The originality of this work lies in the quantitative distinction between the contributions of conduction, convection, and radiation heat transfer in both packed and fluidized beds, based on a CFD-DEM thermal model. The results of the model have been verified using experimental data from the literature, and good agreement has been found. The results show ability for direct comparison under the same conditions, allowing the influence of particle motion on heat transfer between phases to be distinguished. This fills the gap between empirical correlations and numerical calculations for fluidized bed thermal design. The simulations indicate that the heat transfer rate in packed beds is sensitive to the material type of the particles and particle size. While the mechanisms of heat transfer in fluidized beds are more complex due to the motion of particles and the interaction with the fluid phase. Results show that convection was dominant in fluidized beds, with the heat exchange between fluid and particles, while the contribution of the other two mechanisms (conduction and radiation) are decrease and declines from what their contribution to the fixed bed. The findings provide mechanistic insights into thermal transport in multiphase systems and validation data for modifying and developing the design of the fluidization units.

Keywords: Heat transfer; Conduction; Convection; Radiation; Fluidiation

1 Introduction

Packed and fluidized beds find extensive applications in areas of chemical, petrochemical, energy, and environmental engineering because of their large surface area, mixing, and efficient mass and heat transport. These range from catalytic reactors and drying to combustion and gasification systems. Thermal performance of these systems is of crucial importance to their design and optimization since it directly affects reaction rates, energy efficiency, and operational safety [1-4]. Knowledge of the heat transfer mechanisms in these beds continues to be a research priority, particularly under dynamic conditions of fluidization and particle motion. Despite the importance of packed bed operations, surprisingly, there is a lack of research in the area of heat transfer process studies in packed beds, compared with solid-fluid fluidized bed systems [5]. The first theoretical consideration of heat transfer in packed bed systems was represented by a monograph in 1930 by Dittus and Boelter. [6].

* Corresponding author
E-mail address sherko.flamarz@gpu.edu.iq (Instructor).
Peer-reviewed under the responsibility of the University of Garmian.

In packed beds, solid particles remain stationary, and heat transfer predominantly occurs through conduction within the particle matrix, while convection occurs between the interstitial fluid and the particles, and radiation takes place among particle surfaces at higher temperatures. The effective thermal conductivity of packed beds is significantly influenced by factors such as the arrangement of particles, contact resistance, and the porosity of the bed. Various classical models, including those proposed by Zehner-Bauer-Schlünder (ZBS), Yagi and Kunii, have been established to estimate the effective thermal conductivity of packed beds, taking into account both conduction and radiation aspects [7, 8]. In contrast, fluidized beds represent a dynamic, multi-phase environment where particles are suspended within a fluid flow (either liquid or gas). In fluidized beds, the convective heat transfer dominates, driven by vigorous mixing and enhanced surface renewal due to particle movement [9, 10]. The transition from a fixed bed to bubbling and turbulent fluidization results in a sharp increase in heat transfer coefficients, thus enhancing energy transfer. Besides convection, inter-particle conduction during collisions and radiative exchange can also play a crucial role under specific operating conditions.

The analytical and semi-empirical models depend on a range of simplifying assumptions, including uniform particle sizes, homogeneous flow conditions, and idealized interactions between particles. These assumptions can significantly diminish their accuracy in non-ideal situations. Consequently, this leads to a substantial gap in the predictive modeling of thermal transport in real-world systems. Investigative studies on heat transfer within multiphase systems, such as fluidized beds, frequently encounter challenges related to inadequate spatial and temporal resolution, difficulties in monitoring individual particles, and the use of intrusive measurement techniques that may disrupt the flow field. Although empirical correlations, which are based on the Nusselt number and Reynolds number, have offered engineering approximations for heat transfer coefficients [11, 12], they often lack mechanistic understanding and are limited in their applicability across various regimes, scales, and combinations of particles and fluids. A lot of work has been conducted in this field, where experimental researches have essentially tried to establish empirical correlation formulae in order to assess values related to heat transfer [10, 13, and 14]. The design and control of industrial reactors involve some fairly basic principles about heat and mass transfer. Several correlations have, therefore, been developed that describe heat transfer from single particles in packed or fluidized beds and provide estimates of the corresponding coefficients of heat transfer [15-21]. These traditional methods of analysis often work on the macroscopic level to study the behavior of overall heat transfer in the packed and fluidized beds. On the other hand, different techniques have been proposed at the particle scale (microscopic level), to deal with multiphase flow and mainly based on tracing the trajectory of motion and temperature for a single particle in packed or fluidized beds [22-26].

To overcome these challenges, a combination of these two techniques, Computational Fluid Dynamics (CFD) and the Discrete Element Method (DEM), has become an efficient computational method for simulating heat transfer processes on the microscopic level for packed and/or fluidized beds. In this approach, the computational domain representing the fluid phase considers the Navier-Stokes equation and the energy equation, whereas the particles, using the DEM, track their individual motions, which account for inter-particle contact, collisions, and motion [27-31]. This two-way coupling allows detailed resolution of the momentum, mass, and heat transfer between fluid and solid phases, capturing both macro-scale flow behavior and micro-scale particle interactions. The coupled CFD-DEM method has been recognized as a powerful approach to simulate both the fluid flow and various particle-scale heat transfer mechanisms, including convective, conductive, and radiative heat transfer. Many of the CFD-DEM models simulate conductive heat transfer through particle-particle and particle-wall contacts [32, 33], and convective heat transfer between particles and fluid [34-37].

Several research works have used CFD-DEM simulations to study the heat transfer process in granular materials. Zhang et al. [38], where the CFD-DEM simulation of the heat transfer process in randomly packed spheres with low Reynolds number and temperature-dependent fluid properties (hydrogen as the working fluid) was performed. The local distributions of the Nusselt number and the influence of porosity on the temperature profile were analyzed. Quan et al. [39], are studied the packed beds through the CFD-DEM approach, cryogenic hydrogen flow has been modeled, demonstrating the potential of this method to simulate energy storage processes at low temperatures, with a focus on the convective heat and mass transfer between fluid and particles. Tsory et al. [40], are developed a thermal model to predict the effective thermal conductivity for packed beds and various loads. Heat and mass transfer during the melting of a packed bed using a CFD-DEM coupling approach was studied by Baniasadi & Peter [41]. Lu et al. [32] simulated a DEM study of the particle-level contact area forces of granular materials, which affect the thermal conductivity. The effects of thermal radiation on particle-scale heat transfer have also been studied. Wu et al. [42] coupled CFD-DEM with radiation modeling for packed pebble beds, demonstrating that radiation has a significant impact on temperature fields, especially for high-temperature processes, and introduced a set of dimensionless numbers to describe radiation effects.

Compared to packed beds, fluidized beds are characterized by a higher degree of complexity because of the irregular motion of the particles, the presence of bubbles, and the high degree of interaction between the fluid and the particles. CFD-DEM has been successfully employed for this purpose to study its impact on various heat transfer mechanisms. Wang et al. [43], are comprehensively studied fluidized beds for heat transfer analysis, employing CFD-DEM to simulate a bubbling fluidized bed, and experiments were conducted to validate this approach. The study proved that the velocity of the fluid and the size of the particles significantly affect convective heat transfer, and that a fluidized bed is characterized by a multi-peaked particle temperature profile because of collisions. In another study on fluidized beds, Jun and Miaomiao [44], are employed CFD-DEM to simulate a biomass combustion reaction, along with a heat transfer analysis. Although this study was focused on a specific reaction, it proved to be a critical analysis of radiation and convective heat transfer, which are responsible for temperature in a fluidized bed, with a secondary role for particle-to-particle conduction in regions of high concentration. Hoorijani et al. [45] work has also employed CFD-DEM in spouted pulsed fluidized beds, where the flow characteristics and the heat transfer correlation in bi-dispersed particles were evaluated. The work has revealed that the application of external forces, such as pulsed flow, can increase the rates of both convective and radiative heat transfer. Hu et al. [46], are proposed an advanced CFD-DEM analysis, which has also been conducted to evaluate the heat transfer in directly irradiated fluidized beds, demonstrating the influence of the heating conditions on the temperature fields and the various modes of heat transfer under different operating conditions. Gan et al. [47] studied particle-level heat transfer phenomena in packed as well as fluidized beds. Bellan et al. [48] simulated a numerical CFD-DEM study of gas-solid reactors during solar thermal processes. The convective heat transfer study of bubbling fluidized beds using CFD-DEM simulations was conducted by Zhou et al. [36]. The study proposed that convection is more significant than conduction during a bubbling fluidized bed process. The study done by Qiu et al. [49] using CFD-DEM simulations of a bubbling fluidized bed process suggested a dominant role of convection in heat transfer. Other studies done by [50-53] suggested a CFD-DEM coupling model study of the heat transfer, pneumatic conveying system, etc. The role of radiative heat transfer during high-temperature processes using CFD-DEM simulations was studied by Wu et al. [37]. The study concluded that radiative transfer increases the total heat flux significantly.

Nevertheless, few studies have comprehensively addressed all three mechanisms of heat transfer (conduction, convection, and radiation) simultaneously within both packed and fluidized states using a unified CFD-DEM coupling. In this research work, a coupled CFD-DEM simulation is conducted to conduct a comparative analysis of the heat transfer characteristics of packed and fluidized beds under the same conditions. The outcomes clearly indicate that the convective heat transfer coefficient is higher in fluidized beds, the contribution of conduction is lower, and the motion of particles affects the overall heat transfer process. A special focus is given to the effect of particles made of materials aluminum (Al) and Chromium oxide (Cr_2O_3).

The novelty of the current study is in offering a comprehensive and quantitative assessment of the primary heat transfer modes in both packed and fluidized beds through a coupled CFD-DEM simulation approach and thermal model. Differing from previous work that mostly presented the total heat transfer coefficients or concentrated on one heat transfer mode, the current work systematically breaks down the heat transfer process into conduction, convection, and radiation heat transfer modes under the same operating conditions for both packed and fluidized systems. This enables the direct effect of particle motion, such as collisions, circulation, and mixing, to be identified and quantitatively evaluated based on its contribution to interphase heat transfer. Furthermore, the objectives of the current work examine the effect of the most significant operating and material variables, such as particle material properties, particle diameter, fluid velocity, and wall temperature from 100 to 500 °C, to provide a mechanistic understanding of how these variables affect the relative significance of each heat transfer mode. Hence, the results provide numerical validation that fills the gap between empirical heat transfer correlations and accurate CFD-DEM simulations, contributing to enhanced understanding and design optimization of thermal multiphase fluidization systems.

2 Methods and Materials

2. 1 Governing equations for the solid phase

The DEM code (software) is developed in our laboratory [54-57], in which the code works by a mechanism of prediction and correction, where the solver uses the contact method (bi-potential). The Solid phase (particles) is modeled according to the premises adopted in this work; assume that the particles are considered to be rigid throughout the simulation, a hard sphere model, and that the contact between two adjacent particles. The DEM is developed by Cundall & Strack [27]. The DEM provides the opportunity to simulate kinematic and dynamic effects caused by a large number of interacting particles using numerical modeling. In the current work, the DEM solver uses the Non-Smooth Contact Dynamics (NSCD) method, which is employed for short contact with the particles. The DEM is based on Newton's second law of motion, and the particles are assumed to be rigid and impenetrable. Thus, each particle has two motions (translation and rotational) and a governing equation for the solid phase (particle *i*);

$$m_i \frac{dv_i}{dt} = \sum_{j=1}^{x_c} F_{C,ij} + F_{i,B} + F_{i,f} \tag{1}$$

$$I_i \frac{d\omega_i}{dt} = \sum_{j=1}^{x_c} (M_{t,ij} + M_{r,ij}) \quad and \quad I_i = \frac{2}{5} m_i R_i^2 \tag{2}$$

The $F_{i,f}$ represent drag force, which is defined according to Di Felice's drag force model for a particle in a dense system. The Di Felice model is less computationally expensive yet still retains key physics of particle-fluid interactions in dense systems [58]. The drag force is:

$$F_{i,f} = 0.125\pi d_i^2 C_{d,i} \varepsilon_i^{-\chi} \rho_f \left| v_i - v_f \right| \left(v_i - v_f \right) \tag{3}$$

$$C_{d,i} = \left(0.63 + \frac{4.8}{\sqrt{\mathrm{Re}_i}} \right)^2 \cdot \varepsilon_f^{\,2-\left(3.7-0.65 e^{\left(\frac{-(1.5-\log_{10}(\mathrm{Re}_i))^2}{2}\right)}\right)} \quad and \quad \mathrm{Re}_i = \frac{d_i \rho_f \left| v_i - v_f \right|}{\mu_f} \tag{4}$$

$$\chi = 3.7 - 0.65 \exp[-(1.5 - \log_{10} \mathrm{Re}_i)^2 / 2] \tag{5}$$

Where m_i, v_i, d_i, ε_i, Re_i, and ω_i represent mass, translational velocity, diameter, porosity, Reynolds number, and angular velocity of the *i* th particle, respectively, and x_c is the number of candidate particles to interact with particle *i*, and the $F_{C,ij}$ is the elastic contact force between particles use Hertz-Mindlin contact model [59], $F_{i,B}$ is the buoyancy force $C_{d,i}$ is the fluid drag coefficient, μ_f, ρ_f are viscosity and density of the fluid, respectively, and χ is an empirical coefficient. I_i and R_i are the moment of inertia and radius of the particle, respectively. Torque M_{ij} acting on particle *i* by particle *j*, which includes two components ($M_{t,ij}$ and $M_{r,ij}$).

2. 2 Governing equations for fluid phase

The computational platform was established with the Salome platform coupled with the CFD (Code_Saturne), both developed by France's electricity (EDF). The Salome platform provides general-purpose CAD-based software that facilitates pre-processing and post-processing of numerical simulations. The continuum approach (CFD) based on Navier-Stokes equations for incompressible flow, the CFD is used with Code_Saturne, which is based on the Finite Volume Method (FVM) for solving fluid flow problems by discretizing the governing partial differential equations (PDEs) over small parts of the domain known as control volumes [28]. The fluid phase is described by Reynolds-averaged Navier-Stokes equations, and is expressed as;

Conservation of mass (continuity equation)

$$\nabla \cdot v_f = 0 \tag{6}$$

Conservation of momentum

$$\frac{\partial v_f}{\partial t} + (v_f \cdot \nabla) v_f = -\nabla p + \frac{\mu_f \nabla^2 v_f}{\rho_f} + f \tag{7}$$

Where v_f is the velocity of fluid, p is the pressure of fluid, t is time, and f is the external body force per unit mass.

The geometric model was built using Salomé, which is an open-source software platform, where the boundary conditions were also set, and then meshed and discretized to unstructured tetrahedral elements, providing a generic Pre-Processing and Post-Processing environment for numerical simulation. For each particle, the interaction force between fluid and solid is determined, which is the drag force. Although code-Saturne is used as a solver solving the RANS (Reynolds-Averaged Navier-Stokes) equations for incompressible mean flow by using a finite volume discretization method, the CFD code is based on a co-located finite volume method that allows meshes with any type of cell for simulations of the fluid flow [28].

3 Mechanics of CFD-DEM Coupling

The combination of CFD and DEM has been a powerful tool in simulating multiphase systems with fluid-particle interactions in fluidized beds. The method involves the modeling of the fluid phase based on the Navier–Stokes equations and the tracking of individual particles using Newton's equations of motion. Two-way coupling is realized by interphase momentum exchange through drag and buoyancy forces. The coupling methodology can be explained by the following steps; *a*) DEM calculation: compute particle-particle and particle-wall contact forces, and update particle positions and velocities [28], *b*) Data mapping: interpolate particle properties (e.g., position, velocity, volume fraction) onto the CFD mesh, *c*) CFD solver: solve fluid flow equations with updated source terms, including momentum exchange, *d*) Interpolate fluid forces (e.g., drag): onto particles and incorporate them into the next DEM iteration. This iterative process ensures tight coupling and momentum conservation between the two phases.

4 Mechanisms of heat transfer in packed/fluidized beds

Heat transfer occurs by raising the temperature of an object or by energy flow from a higher temperature region to a lower temperature one. Heat energy is transferred from bodies at high temperatures to those at low temperatures, hence transferring energy associated with the motion of molecules, vibration, and rotation of the body. Normally, in a system, heat is conserved and flows from areas where substances exist at high temperatures to those at lower temperatures [60]. In packed beds, heat is transferred primarily through conduction between the particles, with radiation heat transfer at high temperature [61], and contributions from the solid phase. On the other hand, heat transfer in fluidized beds is through convection and radiation, besides the complexity of the particles' interactions and physical processes in the solid phase.

4. 1 Governing equations of heat transfer

The employment of DEM combined with CFD methods improves the prediction of the heat transfer of such systems, since it allows the investigation of all interactions, determining the behavior of the particles, penetration, conduction, and storage in a comprehensive manner. The mechanisms of heat transfer have been studied through simple approaches and models, and by using empirical correlations, which may not be enough to cover the complexity of the processes. When two particles, especially in packed beds with different temperatures, they will begin to exchange heat energy and momentum. Generally, the energy balance for an i particle can be written as,

$$m_i C_{p,i} \frac{dT_i}{dt} = \sum_{j=1}^{n_i} Q_{ij,Cond} + Q_{ij,Conv} + Q_{i,Rad} \tag{8}$$

$$T_{p,i}^{t+\Delta t} = T_{p,i}^{t} + \frac{\Delta t}{m_i C_{p,i}} \left[\sum_{j=1}^{n_i} Q_{ij,Cond} + Q_{ij,Conv} + Q_{i,Rad} \right] \tag{9}$$

Where $C_{p,i}$ is the specific heat of particle i, n_i is the number of particles in contact and exchanging heat energy with particle i, $Q_{ij,Cond}$ is the total conduction heat exchange between particle i and particle j, and particle i with the wall (contact case: the DEM code considers the wall as a particle), $Q_{ij,Conv}$ is convection heat exchange between the particle and the local surrounding fluid, $Q_{ij,Rad}$ is radiation between the particle and the surrounding, and $T_{p,i}^{t+\Delta t}$ represent the mean particle temperature. Different approaches have been developed to describe the contribution of each mechanism of heat transfer, whether in packed or fluidized beds, as follows;

4. 1. 1 Conduction heat transfer

Heat transfer occurs from high-temperature to low-temperature regions because of the interactions among the molecules in the material. It is quantified by thermal conductivity, which measures the propensity of a material to conduct heat. In packed bed applications, this parameter is fundamentally important in the explanation of heat transfer among the solid particles. Thermal contact conductance can be defined as the ratio of the amount of thermal energy transferred through an interface to the extent of temperature gradient existing at that interface, and the contact conductance is calculated at every time step, and takes into account all contacts of a particular particle. It must be recalled once again that the particles are assumed to be non-deformable and impenetrable. The use of Hertz's theory allows for the determination of the contact conductance coefficient ($h_{ij,Cond}$) only, it expresses as,

$$h_{ij,Cond} = 2\lambda_p \left(\frac{3F_{ij,n}a^*}{4E^*}\right)^{\frac{1}{3}} \quad (10)$$

$$Q_{ij,Cond} = h_{ij,Cond}(T_j - T_i) \quad (11)$$

Where $h_{ij,Cond}$ is the coefficient of conductance due to contact between particles i and j, T is the temperature, λ_p is the thermal conductivity of solid particles, $F_{ij,n}$ is a normal component of contact force, a^* is equivalent radius, and E^* is the equivalent Young modulus of particles in contact.

4. 1. 2 Convection heat transfer

This mechanism occurs through the particle-fluid interface, the heat energy exchange when the fluid (liquid or gas) flows through the bed. The rate of convection is affected by many parameters, like the temperature difference between the solid phase and fluid phase, fluid velocity, and thermal capacity of the fluid. Oftentimes, convection heat transfer is calculated through an equation.

$$Q_{ij,Conv} = h_{iif} S_i (T_{if} - T_i) \quad (12)$$

Where h_{if} is the convective heat transfer coefficient, S_i is the surface area of the particle contact with fluid, T_{if} is the fluid temperature surrounding the particle i. Many empirical correlations and equations have been proposed to estimate the convective heat transfer coefficient from the calculation of Nusselt number (Nu) [10, 13-15], which is calculated by;

$$Nu = \frac{h_{if} d_i}{k_f} = 2.0 + a\,\mathrm{Re}_i^b\,\mathrm{Pr}^{\frac{1}{3}} \quad and \quad \mathrm{Pr} = \frac{C_{p,f}\,\mu_f}{k_f} \quad (13)$$

Where Pr is the Prandtl number and represents the fluid properties, a and b are two parameters that need to be estimated. Kunii and Levenspiel [10] suggest b = 0.5, and a is in the range (0.6-1.8). According to recent literature data, the value of a is estimated around 1.2, so in the present work (a=1.2).

4. 1. 3 Radiation heat transfer

Regarding radiation, it is heat transfer by electromagnetic waves between bodies at temperatures greater than 273°C. This energy transfer at the walls to the bed or vice versa within packed beds is so vital and significant that it tends to cause an energy transfer even between solid particles by agglomeration. The radiation heat transfer can be written as,

$$Q_{i,Rad} = \sigma S_i e_i (T_{if}^4 - T_i^4) \quad (14)$$

Where σ =5.67*10^{-8} w/(m^2.K^4) is Stefan-Boltzman constant, and e_i is the emissivity of a sphere particle.

4. 2 Selection of particle materials

In this study, Aluminium (Al) and Chromium oxide (Cr_2O_3) particles were utilized to simulate two highly distinct classes of solids with highly disparate thermal and physical characteristics. The aluminium particle is a light metal particle with high thermal conductivity, enabling very quick heat transfer, high thermal responsiveness in the fluidized bed, and low emissivity. On the other hand, chromium oxide has low thermal conductivity, high density with a more insulating nature, a reduced thermal response rate, and high emissivity. This seeming disparity constitutes a handy basis for investigating the influence of particle density and thermal conductivity on interphase energy transfer, temperature distribution of the particle, and overall heat transfer performance. Moreover, aluminium and chromium oxide also have widespread applications in industrial applications such as metallurgy, thermal energy storage, catalysis, and refractory coating, which makes their selection of great utility in real operations.

5 Strategy of CFD-DEM coupling with thermal model

Until now, there is no standard algorithm for CFD-DEM coupling strategies, and the existing approaches have specific limitations and challenges that must be solved. Hence, the information exchange takes place through the following mechanism;

- Fluid solver provides local fluid velocity, temperature, and pressure to the DEM solver.
- DEM solver computes void fraction, location, and particle velocities.
- Momentum exchange: fluid drag ($F_{i,f}$) and pressure gradient forces on particles, plus the reaction momentum to the fluid.
- Heat exchange: The convection term at the fluid-particle interface, plus the contact-based conduction, and radiation between the particles.

6 Results and Discussion

Modeling of solid-fluid interaction, mass and heat transfer across the phases, and wall structures in packed and fluidized beds is extremely complicated. The numerical simulation will help to understand complex interactions based on analysis and knowledge regarding heat transfer improvement.

6. 1 Validation of CFD-DEM combined with thermal model

In this part, to check the validity of the thermal approach, which includes the coupling of the CFD-DEM combined with a thermal model, the time dependence of the average temperature of the mean particles during the cooling, as shown in Fig. 1, the average particle temperature decreases over time at all tested air velocities, confirming the expected cooling trend. The results from the CFD-DEM simulations align closely with experimental data for air velocities of 1.2 m/s and 1.54 m/s, validating that the numerical model accurately simulates the primary convective heat transfer processes. Additionally, as the air velocity increases, the cooling rate also rises. This is due to the increase in the particle Reynolds number, which enhances the convective heat transfer coefficient and, consequently, improves heat transfer from the particles. The cooling process was checked against the experimental findings obtained by Patil et al. [23]. The simulation of the fluidization process was carried out on a pseudo-2D fluidized bed containing glass particles with a diameter of 1mm. The bed dimensions were 8 cm in width, 20 cm in height, and 1.5 cm in depth. The height of the bed at rest (H_o= 42 cm), and the top of the container is closed to prevent overflow of the particles. The particle and fluid properties are tabulated in Table 1. The air properties were assumed constant in all simulations. The particles started at a temperature of 80°C, and then a steady airflow of 20°C was blown from the bottom inlet with different velocities (v_f = 1.2, 1.54, and 1.71 m/s). Fluidization and convective cooling of the particles in the direction of the airflow took place for 22 s.

For Fig. 1, the average particle temperature decreases with time for all air velocities, which verifies the expected cooling trend. The CFD-DEM simulation results match well with the experimental data for air velocities of 1.2 and 1.54 m/s, which validates that the numerical model is able to simulate the major convective heat transfer processes correctly. As the air velocity increases, the cooling rate also increases due to the rise in the particle Reynolds number, which enhances the convective heat transfer coefficient and thus the heat transfer from the particles.

There is a slight deviation between the numerical simulation and experimental data at the highest air velocity (v_f = 1.71 m/s), particularly in the initial stage, where the numerical simulation overestimates the cooling rate. This might be because of the increased turbulence and air flow fluctuations at higher velocities, which are not considered in the simplified heat transfer equations. As the temperature difference reduces with time, the cooling rate reduces, and the numerical simulation and experimental data match well again.

Numerical results compare reasonably well with experimental measurements throughout the cooling period, except for minor deviations at later times. In general, this close correspondence confirms the applicability of the CFD-DEM thermal model to predict transient heat transfer in fluidized beds.

Table 1: Properties of the solid particles (glass) and the fluid (air) used in the simulations.

Symbol	Parameter	Value
d_p	Particle diameter (mm)	1.0
H_o	Bed height (initial) (mm)	420
ρ_p	Density (kg/m^3)	2500
E	Young's modulus (Gpa)	70.0
ν	Poisson's ratio (-)	0.35
μ_s	Coefficient of friction (-)	0.30
Cp	Heat capacity (J/(kg.K))	840
λ_p	Thermal conductivity (W/(m.K))	1.40
ρ_f	Fluid density (kg/m^3)	1.177
μ_f	Viscosity (kg/m.s)	1.85×10^{-5}
C_f	Heat capacity (J/(kg.K))	1010
λ_f	Fluid thermal conductivity (W/(m.K))	0.262
Δt	Time step for fluidized bed [s]	$5*10^{-5}$

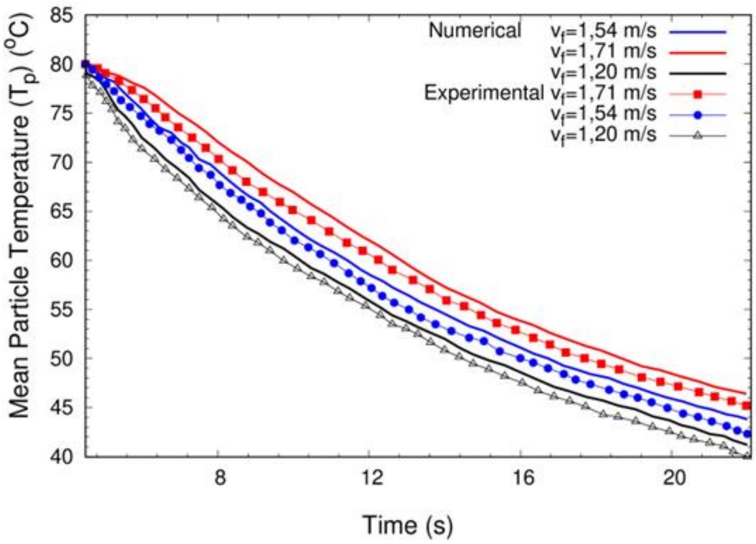

Figure 1: Comparison between the CFD-DEM simulation results and experimental data, showing the evolution of the mean particle temperature with time during the cooling process.

6. 2 Modeling the heat transfer in packed beds

Modeling for packed beds consists of two cases: case 1, the bed material (solid phase) is composed of aluminum (Al), and case 2, from chromium oxide (Cr_2O_3). The properties are shown in Table 2. The base of the column (inlet) is maintained at constant wall temperature for a range of temperatures (100-500 °C). The particles are considered hard spheres and non-penetrable. The particles are placed in a column with a diameter (D = 0.51 m) and height (H = 0.75 m). For packed beds simulation, a bed of thickness (H_o=400 mm) with particle diameter (d_p= 3 mm), and the column walls, bed particles, and inlet fluid were at 20 °C. In the modeling, the fluid flow is passed upward by superficial velocity (0.08 m/s) through the bed.

Table 2: Physical properties of Aluminum and Chromium oxide particles and relevant CFD-DEM simulation parameters.

Material property			
Symbol	**Parameter**	**Aluminum (value)**	**Chromium oxide (value)**
ρ_p	Density (kg/m^3)	2700	5210
λ_p	Thermal conductivity (W/(m.K))	237	32.94
C_p	Heat capacity (J/(kg.K))	900	1676
e_i	Emissivity (-)	0.20	0.85
E	Young's modulus (Gpa)	69.0	255
ν	Poisson's ratio (-)	0.35	0.25
t	Simulation time for packed bed (s)	70.0	
t	Simulation time for fluidized bed (s)	20.0	
Δt	Time step for packed bed (s)	$1*10^{-4}$	
Δt	Time step for fluidized bed, Δt (s)	$5*10^{-5}$	
d_p	Particle diameter (mm)	3 for packed bed, 1.5 for fluidized bed	

6. 3 Packed Bed Results

In the packed-bed cases, at all wall temperatures, an initial increase in particle temperature is observed, followed by a gradual approach to thermal equilibrium. This transient thermal response arises from the temperature difference between the heated wall and the cooler particles and fluid phase. The heat transfer process is effectively captured by the CFD-DEM, which accounts for conduction between the particles and the wall, convection between the particles and the fluid, and heat transfer through contact conduction among the particles.

Fig. 2 illustrates the influence of wall temperature on the mean particle temperature in a packed bed. With the increase in wall temperature, the temperature difference between the wall and particles becomes greater, thus promoting the heat transfer rate and speeding up the heating process of particles, particularly in the initial period. When the inlet wall temperature T_w=100°C, the particle temperature reaches equilibrium rapidly but remains slightly lower than the wall temperature because of the convective resistance and poor heat transfer in the interstitial fluid. When T_w= 500°C, it takes a longer time for the system to attain equilibrium because of the greater thermal energy involved and the higher thermal inertia of particles. Moreover, the internal temperature difference becomes greater with the increase of wall temperature, thus causing the non-uniform heating of the packed bed and prolonging the process of thermal homogenization.

The temperature evaluation in the beds indicates different characteristics for aluminum (Al) and chromium oxide (Cr_2O_3) particles based on their thermal properties. For the aluminum particles (Fig. 2a), the temperatures of the particles attain equilibrium in 20 seconds of simulation time, mainly because of the high thermal conductivity of aluminum, which favors quick conduction of heat from particle to particle and particle to wall. For the Cr_2O_3 bed (Fig. 2b), the temperature dynamics indicate that at 500°C, the temperatures of the particles increase rapidly in the first 30 seconds of simulation time before reaching equilibrium, whereas at 100°C, the heating process is slower but attains equilibrium faster at a lower temperature. This is because of the lower thermal conductivity of Cr_2O_3, which resists conduction of heat from particle to particle and from particle to wall, with higher temperature differences at 500°C favoring higher initial rates of heat flux. This behavior is attributed to conduction-driven heat transfer, where contact conductance and wall conduction limit heat transfer efficiency. This may be attributed to the high thermal conductivity of the aluminum that makes up the bed material.

For aluminum particles (Fig. 3a), the value of conductive heat transfer rises sharply with time and wall temperature, reaching about 15 W at a wall temperature of 500 °C, thus making conduction the principal mode of heat transfer. This sharp rise in conductive heat transfer takes place mainly in the first 5-10 seconds of the simulation process, which corresponds to the time when the temperature difference between the wall and the neighboring particles is maximum. The high value of thermal conductivity and diffusivity of aluminum facilitates easy heat transfer from particle to particle and from the wall to the particles, thus making it possible for the heat to spread rapidly from the heated wall to the neighboring particles. When the particles in the vicinity of the wall get heated, and the temperature difference reduces, the rate of heat transfer by conduction also gradually becomes stable, tending towards a quasi-steady state.

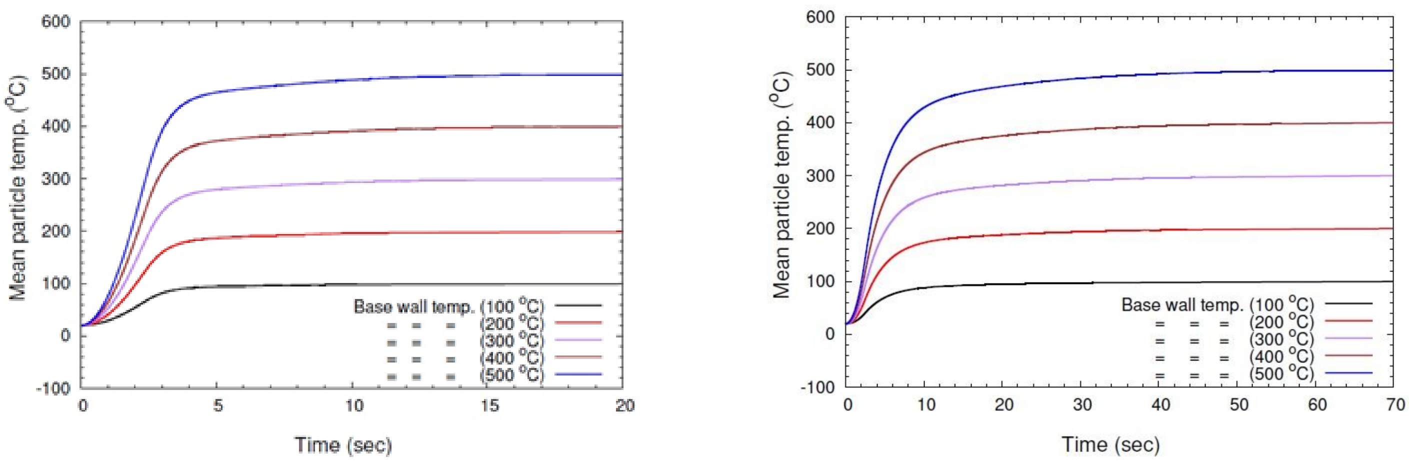

(a) (b)

Figure 2: Temporal evolution of the average particle temperature in a packed bed as predicted by CFD-DEM simulations for various particle materials: (a) Aluminum (Al) particles, which respond very quickly to temperature changes due to their high thermal conductivity, and (b) Chromium oxide (Cr_2O_3) particles, which respond relatively slowly to temperature changes due to their lower thermal conductivity.

Furthermore, the Fig. (3 b) chromium oxide (Cr_2O_3) packed bed has been observed to have a significantly lower conductive heat transfer rate, with a maximum of approximately 2 W under the same thermal boundary conditions, mainly because of the lower thermal conductivity of chromium oxide compared to metals such as aluminum. In a packed bed, the heat transfer by conduction is primarily between particles, and the reduced contact area between Cr_2O_3 particles further reduces the heat transfer. Consequently, the process of heat transfer in the bed becomes more diffusive, where the heat relies on spreading rather than conduction, which slows down the process. This is why there is a timescale involved, where temperature changes take up to 60 seconds.

Fig. 3 (a, b) depicts that, for the same thermal boundary conditions, the aluminum-packed bed has a higher conductive heat transfer rate because of its high thermal conductivity and effective particle contact arrangement, which enables fast heat transfer in the bed. This example illustrates the importance of particle properties in heat transfer rates in a packed bed, where particles with low conductivity need either more time or a higher fluid velocity or particle motion to enable effective thermal homogenization.

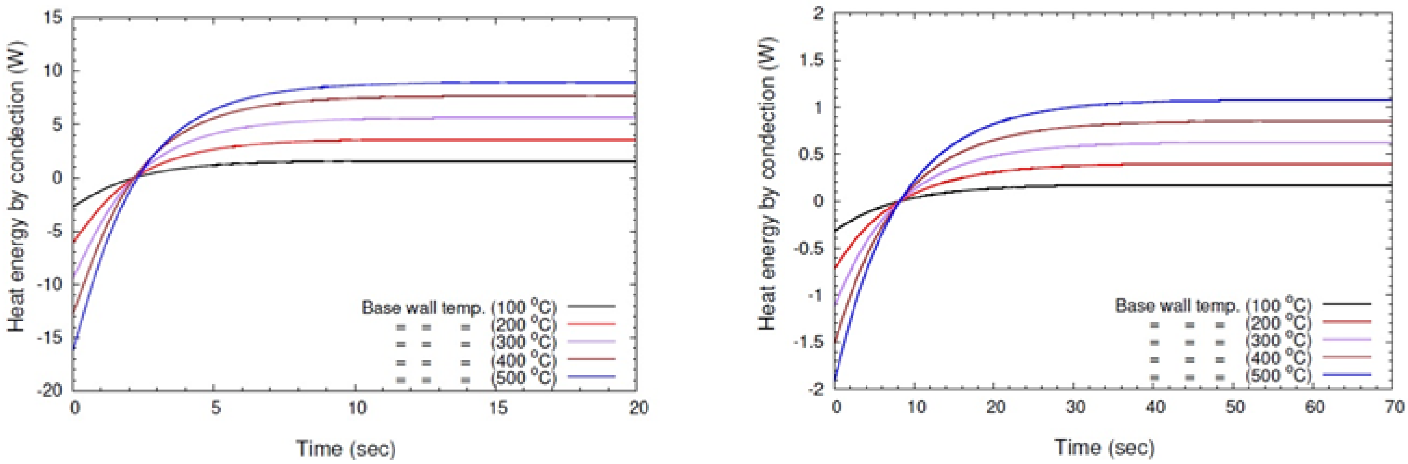

(a) **(b)**

Figure 3: Temporal development of conductive heat transfer in a packed bed of various particle materials: (a) aluminum (Al) particles and (b) chromium oxide (Cr_2O_3) particles. "The above figure illustrates the development of heat conduction through the points of contact between the particles with time, emphasizing the effect of the particle material on the rate of temperature distribution in the bed."

A comparison of the results of simulations in Fig. 4 indicates that particle material has a significant effect on both the value and time dependence of convective heat transfer in fluid-solid packed beds. Aluminum particles, with high thermal conductivity (237 W/m.K), demonstrate a sharp initial increase in convective heat transfer (Fig. 4 a), reaching approximately 60,000 W in 20 s at a boundary temperature of 500°C. This is due to the fact that heat transfer occurs rapidly into the particle bulk, causing a sharp increase in particle temperature and a subsequent decrease in the fluid-particle temperature difference, which makes convective heat transfer less favorable in the long run. Chromium oxide particles (Fig. 4 b), with lower thermal conductivity (32.94 W/m.K), demonstrate a slower heating process; with a larger fluid-particle temperature difference sustained over a longer period of time. Consequently, convective heat transfer increases cumulatively, eventually reaching 120,000 W at 70 s.

This allows for sustained temperature gradients and prolonged convective heat flux, making convection the dominant heat transfer mode for materials with low conductivity. These findings underscore the relationship between particle properties and heat exchange conditions, indicating that aluminum is suitable for quick temperature adjustments, while chromium oxide is better for applications requiring sustained thermal stress.

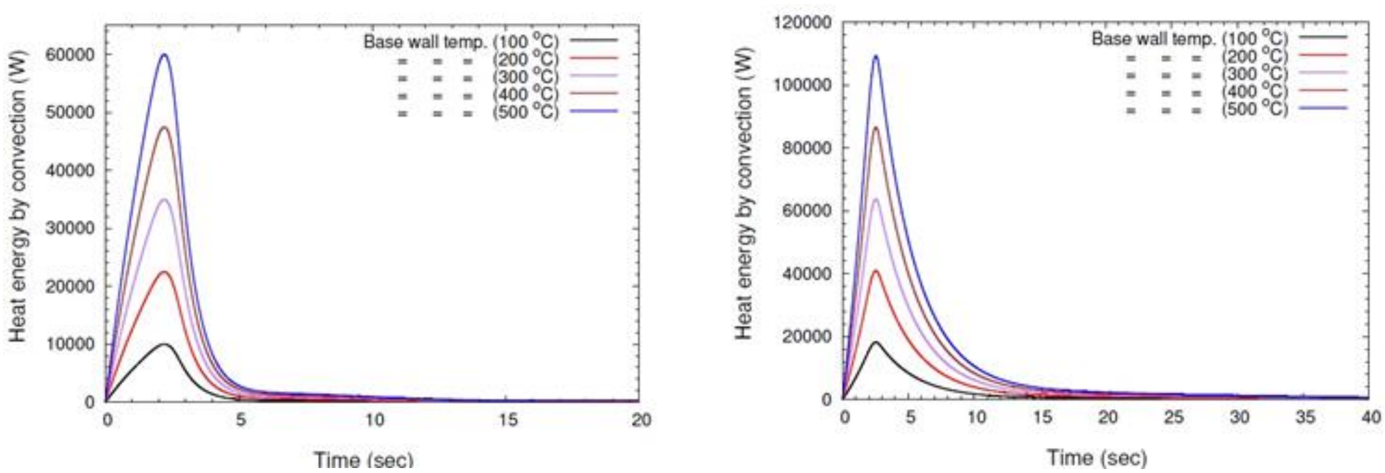

(a) **(b)**

Figure 4: Temporal evolution of convective heat transfer in packed beds containing different particle materials: (a) aluminum (Al) particles and (b) chromium oxide (Cr_2O_3) particles. The figure shows the variation of heat transfer over time, highlighting the influence of particle thermal properties on the rate and distribution of convective heat transfer within the packed bed.

The role of radiation heat transfer in a packed bed is highly dependent on the temperature and thermal and optical properties of the particles. In the case of the aluminum packed bed, as depicted in Fig. 5(a), the contribution of radiation heat transfer is minimal at lower wall temperatures (100-200°C), with a maximum heat energy of less than 0.5 W, due to the low emissivity of aluminum and the fact that reflected radiation from surfaces is not a major source of radiation heat transfer at moderate temperatures. However, at higher wall temperatures of 400°C and above, the contribution of radiation heat transfer increases dramatically to about 3.5 W at 500°C. This is because radiation heat transfer is highly temperature-dependent (T^4), resulting in a substantial increase in radiative flux at higher temperatures, even with low emissivity materials such as aluminum. For a packed bed of higher-emissivity materials such as chromium oxide, the contribution of radiation heat transfer would be more substantial at lower temperatures.

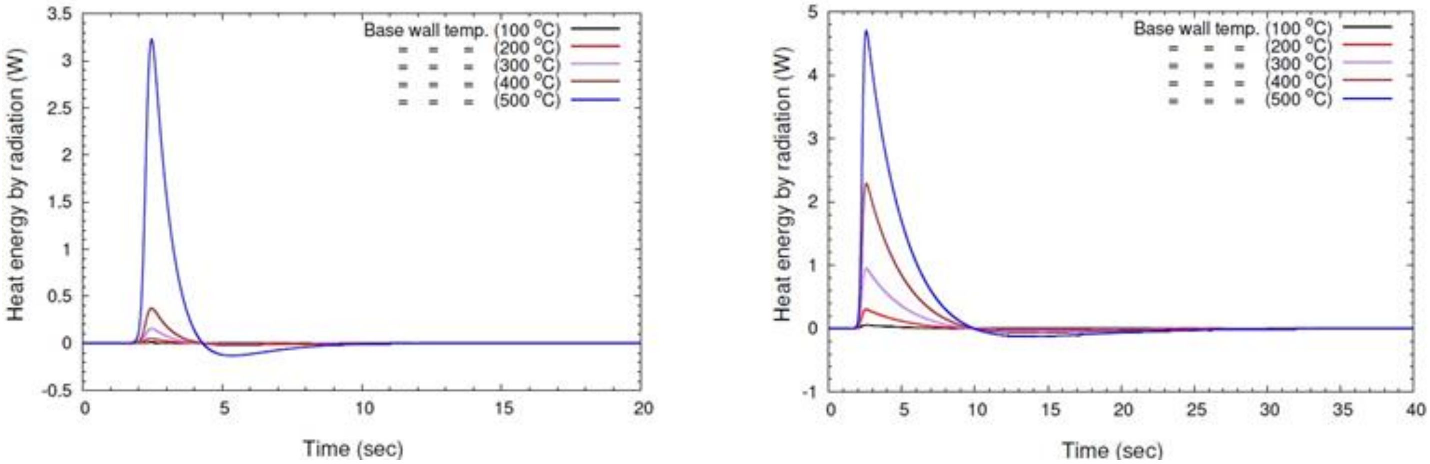

(a) **(b)**

Figure 5: Time variation of radiative heat transfer in packed beds with different particles: (a) aluminum (Al) and (b) chromium oxide (Cr_2O_3). The above graphs show the variation of radiative heat flux with time, emphasizing the effect of the material of the particles on the radiative heat transfer in the packed bed.

Conversely, Fig. (5b) illustrates the packed bed of chromium oxide particles, where the radiative heat transfer is highly dependent on the wall temperature. At higher wall temperatures (such as 500 °C), the total radiative heat flux increases significantly in the first 10-15 s, exceeding 5 W before reaching a steady state. This is mainly attributed to the high emissivity of chromium oxide (e_i=0.85), which increases the radiative heat transfer, and its low thermal conductivity, which reduces the conductive heat loss. Additionally, the large absorption coefficient leads to the penetration of radiation into the particle volume, which increases the volumetric energy transfer. Therefore, the combined effects of these properties lead to the rapid accumulation of radiative heat in the bed. The findings clearly indicate the important role of particle materials in determining the efficiency of heat transfer in multiphase systems. The results are in good agreement with the experimental results in the literature [62-64].

6. 4 Modeling the heat transfer in fluidized beds

As mentioned for packed beds, the modeling for fluidized beds consists of two cases: case 1, the bed material (solid phase) is composed of aluminum (Al), and case 2, the bed is composed of chromium oxide (Cr_2O_3). The material properties are detailed in Table 1. The base temperature of the column (inlet) is maintained at constant wall temperature for a range of temperatures (100-500 ºC). The particles are considered hard spheres and non-penetrable. The particles are placed in a column with a diameter (D = 51 mm) and height (H = 0.75 m). The fluidized beds were packed with particles (solid phase) with a thickness (H_o= 100 mm) and particle diameter (d_p= 1.5 mm), the inlet fluid temperature is 20 ºC, and fluid flow is passed upward over a range of superficial velocities (0.08, 0.12, and 0.16 m/s) through the bed.

6. 5 Fluidized Beds Results

In the fluidized bed, the fluid flows from the base of the fluidizing column upward through the bed; the velocity of the fluid significantly affects heat transfer. In this part of the study, three different interfacial velocities (0.08, 0.12, and 0.16 m/s) were used; the bed, fluid, and walls are initially having a temperature of 20 ºC, and the fluidizing fluid will heat the particles. The particles experience frequent collisions and heat exchange between themselves and with the cooler fluid in the column. Over simulation time, the average bed temperature remains close to the maintained temperature of the inlet wall (base wall).

The temperature development of Aluminum particles with a superficial fluid velocity of 0.08 m/s is shown in Fig. 6 a. It can be seen that the temperature of the particles increases rapidly in the first 5 seconds of heating. This is mainly due to the high thermal conductivity of aluminum (237 W/m·K), which ensures efficient conduction of heat from the heated wall to the particles. Fast heat propagation in the particles due to contact conduction and the surrounding fluid ensures that the bed heats up rapidly. On the other hand, Fig. 6 b shows the temperature development of chromium Oxide particles under the same fluidization process. Due to the low thermal conductivity of chromium Oxide (32.94

W/m·K), the heat transfer from the wall to the particles is slow. As a result, the initial heating of the bed is delayed, and the bed takes time to attain thermal homogeneity.

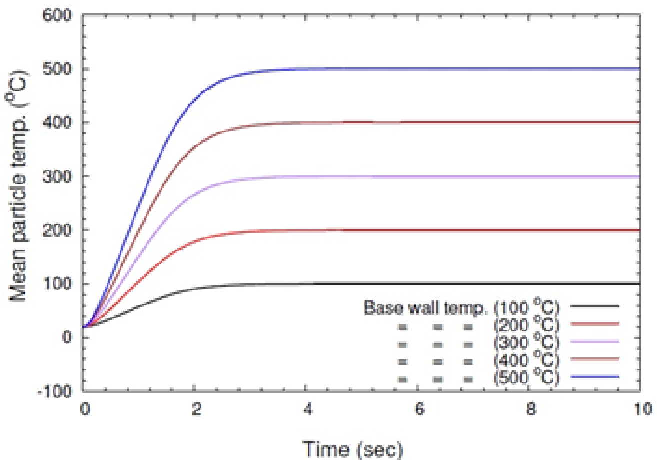

(a)

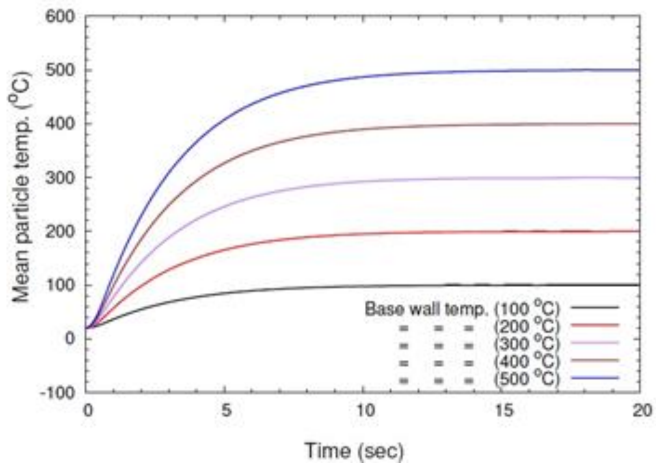

(b)

Figure 6: Temporal development of mean particle temperatures in fluidized beds with a superficial gas velocity of 0.08 m/s. The comparison is made for beds of (a) aluminum (Al) particles and (b) chromium oxide (Cr_2O_3) particles. The figure illustrates the effect of particle material on the heat transfer process dynamics, where the temperature drops faster in the Al bed due to its higher thermal conductivity, and the Cr_2O_3 bed cools more slowly. The obtained data confirm the combined effect of particle properties and fluidization on the heat transfer process in fluid-solid systems.

Fig. (6 a) is revealed the Aluminum particles under a superficial fluid velocity of 0.08 m/s, which showed a more rapid temperature rise compared to Chromium Oxide Fig. (6 b), the effect that was particularly noticeable within the first 5 seconds of heating. This is due to Aluminum's high thermal conductivity (237 W/m.K), which allows effective heat transfer from the heated wall to the particles. In contrast, Chromium Oxide exhibited a much lower thermal conductivity (32.94 W/m.K), showing retarded heat propagation through the bed, while at a superficial fluid velocity of 0.12 m/s (Fig. 7), both particle systems Fig. 7 (a, b) showed improved fluidization and heat transfer compared to the case of 0.08 m/s. However, the relative difference in temperature response persisted.

With the increased inlet fluid velocity of 0.12 m/s (Fig. 7), the Aluminum and Chromium Oxide particles both show better fluidization and increased heat transfer rates than in the 0.08 m/s scenario. The increased fluid velocity leads to stronger convective currents, which in turn reduce the local temperature gradients in the bed and increase the rate of heat transfer. However, the natural thermal properties of the particles again dominate the rate of temperature increase, with Aluminum particles still increasing in temperature faster than Chromium Oxide particles, and the lower-conductivity particles still lagging despite the increased fluid motion.

In summary, the above observations clearly show that:

- The thermal conductivity of the material dominates the initial heat transfer process in the bed, with higher conductivity particles (Aluminum) increasing in temperature faster.
- The superficial fluid velocity increases convective transport, leading to increased heat transfer rates and fluidization, but does not completely suppress the effect of material properties.
- The combined effect of conduction between particle contacts and convective transport by the fluid determines the transient temperature behavior in fluidized beds.

At the highest inlet fluid velocity of 0.16 m/s (Fig. 7), there is highly intensified particle motion for both Aluminum and Chromium Oxide, resulting in high mixing and particle circulation. The high hydrodynamic activity increases the convective heat transfer between the fluid and particles and constantly resurfaces the particles in contact with the heated wall region, thus reducing temperature gradients in the bed. However, Aluminum particles demonstrate better thermal performance (Fig. 7a) than Chromium Oxide particles (Fig. 7b) under similar mixing conditions, as Aluminum particles reach steady-state temperature faster than Chromium Oxide particles. This is primarily due to Aluminum's higher thermal conductivity, which enables faster heat diffusion inside the Aluminum particles, causing the particle core temperature to quickly approach the wall temperature. Conversely, Chromium Oxide particles display a slower temperature increase with a lower final temperature level, reflecting slower heat diffusion inside Chromium Oxide particles because of their lower thermal conductivity.

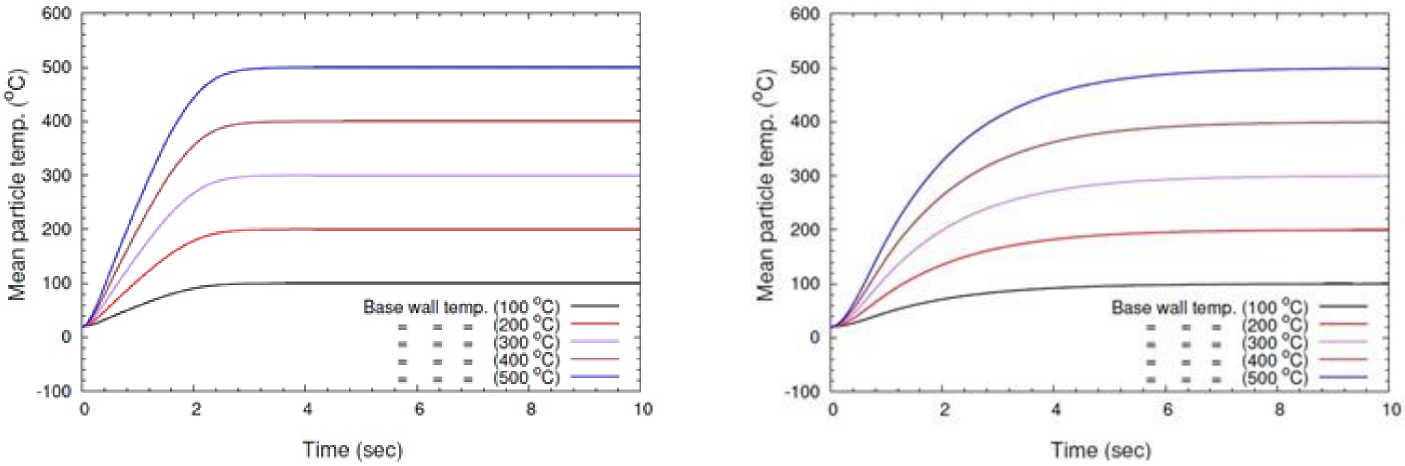

(a) **(b)**

Figure 7: Temporal development of mean particle temperatures in fluidized beds with a superficial gas velocity of 0.12 m/s. The comparison is made for beds of (a) aluminum (Al) particles and (b) chromium oxide (Cr_2O_3) particles. The figure illustrates the effect of particle material on the heat transfer process dynamics, where the temperature drops faster in the Al bed due to its higher thermal conductivity, and the Cr_2O_3 bed cools more slowly. The obtained data confirm the combined effect of particle properties and fluidization on the heat transfer process in fluid-solid systems.

As a result, although the convective heat transfer coefficient increases with velocity, the material-specific internal conduction resistance becomes the most important limiting factor for Chromium Oxide. In terms of quantitative results, the average temperature of Aluminum particles reaches a steady-state value close to the 500 °C wall temperature in about 10 seconds, while Chromium Oxide particles are still far below that value, especially at higher base temperatures, thus verifying that the material properties of the particles have a strong influence on the heating rate even for the same fluidization and mixing process.

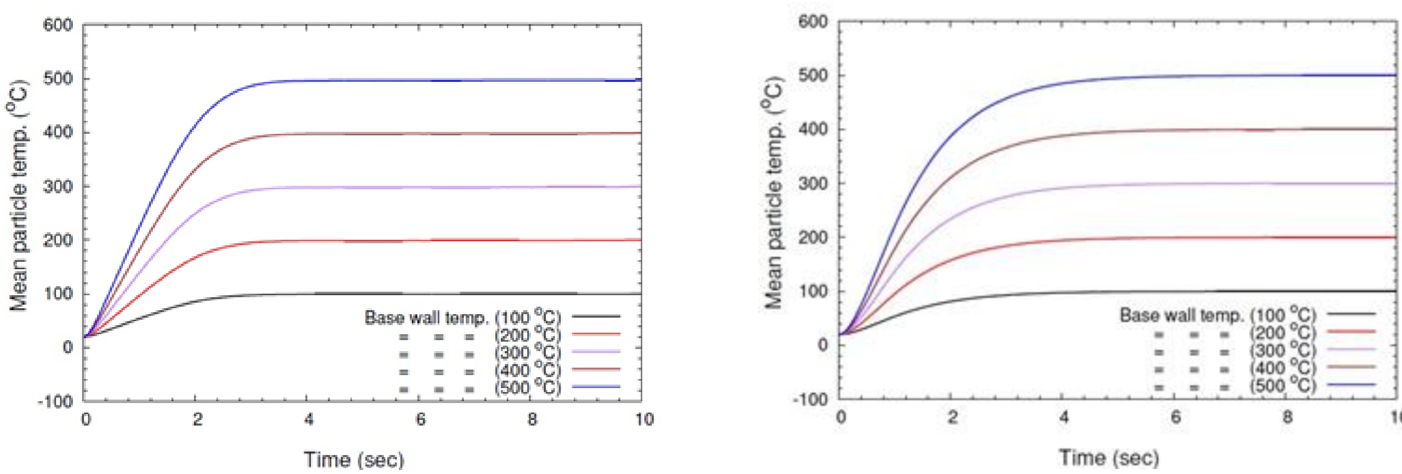

(a) **(b)**

Figure 8: Temporal development of mean particle temperatures in fluidized beds with a superficial gas velocity of 0.16 m/s. The comparison is made for beds of (a) aluminum (Al) particles and (b) chromium oxide (Cr_2O_3) particles. The figure illustrates the effect of particle material on the heat transfer process dynamics, where the temperature drops faster in the Al bed due to its higher thermal conductivity, and the Cr_2O_3 bed cools more slowly. The obtained data confirm the combined effect of particle properties and fluidization on the heat transfer process in fluid-solid systems.

Figs. (9a, 10a, and 11a) show the conduction heat transfer energy distributions of aluminum particles at three inlet velocities (v_f = 0.08, 0.12, and 0.16 m/s). The large conduction heat transfer values in these figures are primarily due to the large thermal conductivity of aluminum (237 W/m·K). As the wall temperature rises, the temperature difference between the hot wall and the particle bed becomes more pronounced, leading to a large conductive heat flux. Hence, at 500 °C, the conduction heat transfer has a maximum peak value of approximately 1.5 W, which clearly reveals a strong conduction-dominated transfer process in the vicinity of the hot wall. Moreover, the large temporal variations, especially in the early fluidization period, are due to the large particle motion and frequent changes in the contact point network, where continuous collisions cause the frequent formation and disruption of conductive paths. Conversely, at lower wall temperatures (100-200 °C), the intensity of thermal driving force is lower, resulting in lower conduction intensity, and the conduction curves gradually tend towards a quasi-steady state after the transient regime as the bed hydrodynamics stabilize.

Similarly, Figs. (9b, 10b, and 11b) present the conduction heat transfer distribution for chromium oxide particles under the same conditions; however, the contribution of conduction heat transfer is substantially lower owing to the lower thermal conductivity of chromium oxide (32.94 W/m·K), which hinders the diffusion of heat. Consequently, even at 500 °C, the conduction heat transfer is lower and peaks at merely 0.35 W, thereby establishing that the conduction process is largely dependent on the material properties of the particles. In summary, the above findings establish that the conduction heat transfer is higher at higher wall temperatures owing to higher thermal forces, whereas the extent of temporal variation is dependent on the particle dynamics, and the principal controlling parameter for conduction heat transfer is the inherent thermal conductivity of the solid material.

Furthermore, these profiles demonstrate more consistent trends and reduced time-related fluctuations, suggesting a slower thermal response and a less dynamic conduction behavior. The negative peaks in Figs. (9, 10, and 11) indicate that the particle (*i*) is losing heat energy to other particles through conduction.

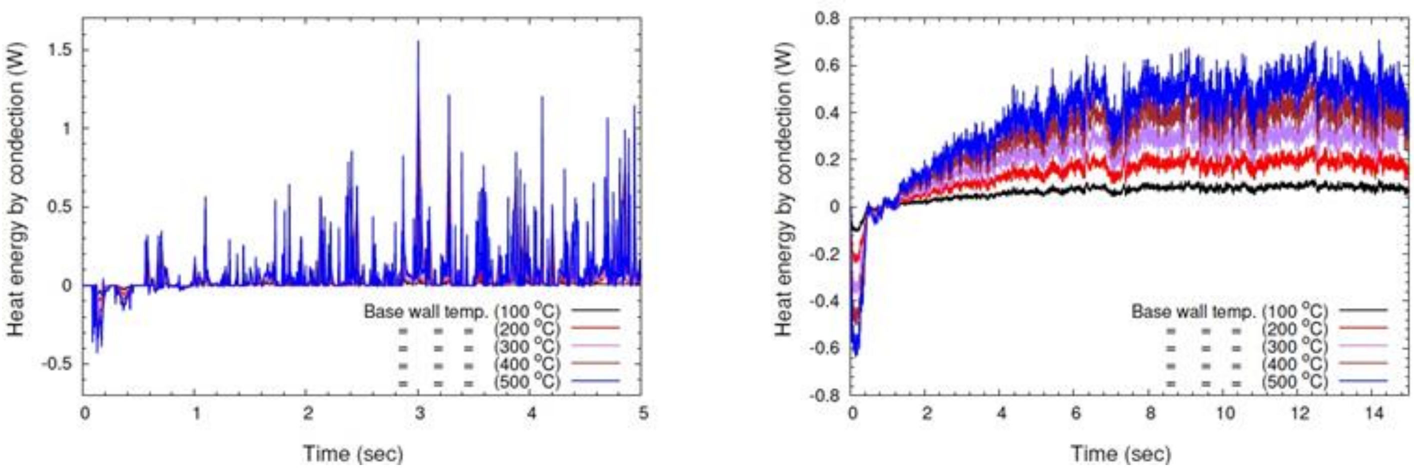

(a) **(b)**

Figure 9: Temporal development of conductive heat transfer in fluidized beds of (a) aluminum (Al) particles and (b) chromium oxide (Cr_2O_3) particles at a superficial fluid velocity of 0.08 m/s. The graph above shows the conductive heat transfer with time for the two types of particle materials, indicating the effect of the particles' properties on the heat transfer process in the bed.

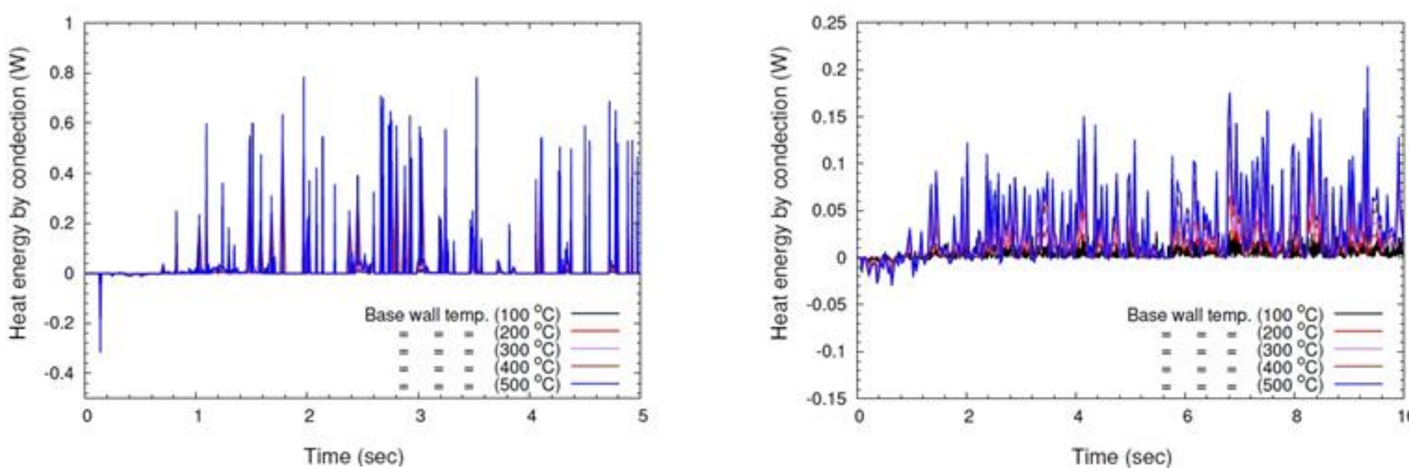

(a) **(b)**

Figure 10: Temporal development of conductive heat transfer in fluidized beds of (a) aluminum (Al) particles and (b) chromium oxide (Cr_2O_3) particles at a superficial fluid velocity of 0.12 m/s. The graph above shows the conductive heat transfer with time for the two types of particle materials, indicating the effect of the particles' properties on the heat transfer process in the bed.

With a low inlet fluid velocity of 0.08 m/s (Fig. 12), the convective heat transfer from chromium oxide particles is approximately 4800 W at a wall temperature of 500 °C (Fig. 12 b), while that from aluminum particles is only about 2700 W (Fig. 12 a). The main reason for this difference is the different thermal characteristics of the two materials. The chromium oxide particles are likely to conserve heat and have a larger temperature gradient between the particle surface and the fluid, thus increasing the driving force for convective heat transfer. However, aluminum has a much higher thermal conductivity, which enables the heat to propagate quickly through the particle, causing the particle temperature to become relatively uniform. Consequently, the temperature difference between the particle surface and the fluid becomes smaller, thus reducing the convective heat transfer even if the flow conditions are improved. When the superficial velocity is raised to 0.12 m/s (Fig. 13), the convective heat transfer coefficient increases because of the increased relative motion between the fluid and particles, which is likely to improve convection.

Nevertheless, the advantage of this velocity increase is more pronounced in the case of chromium oxide, whose particles maintain greater temperature differences and have the ability to continuously transport the stored heat energy from the heated wall region to the bulk bed. As such, the convective heat transfer coefficient significantly rises to approximately 7400 W (Fig. 13 a). On the other hand, the aluminum particles continue to maintain a value of approximately 2700 W, which suggests that the convective heat transfer in this situation is not mainly restricted by the heat transfer coefficient but by the diminished temperature driving force due to the fast thermal equilibration process.

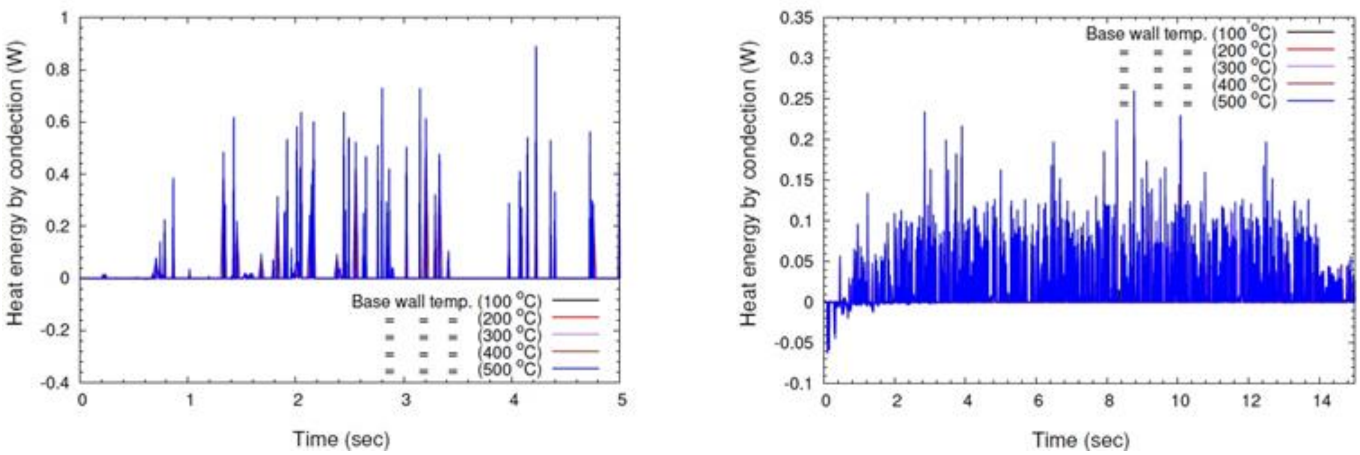

(a) **(b)**

Figure 11: Temporal development of conductive heat transfer in fluidized beds of (a) aluminum (Al) particles and (b) chromium oxide (Cr_2O_3) particles at a superficial fluid velocity of 0.16 m/s. The graph above shows the conductive heat transfer with time for the two types of particle materials, indicating the effect of the particles' properties on the heat transfer process in the bed.

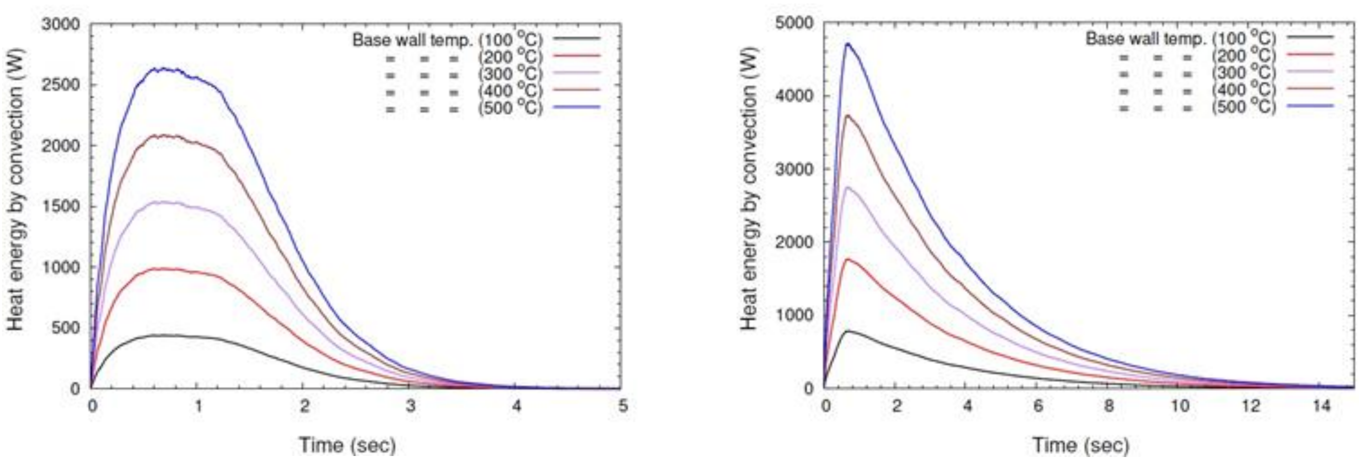

(a) **(b)**

Figure 12: Illustration of the temporal development of convective heat transfer in fluidized beds of (a) aluminum (Al) particles and (b) chromium oxide (Cr_2O_3) particles. The computations were performed at an inlet fluid velocity of 0.08 m/s. The differences in heat transfer characteristics based on the properties of the particles are emphasized in the figure, illustrating the development of the convective process with time.

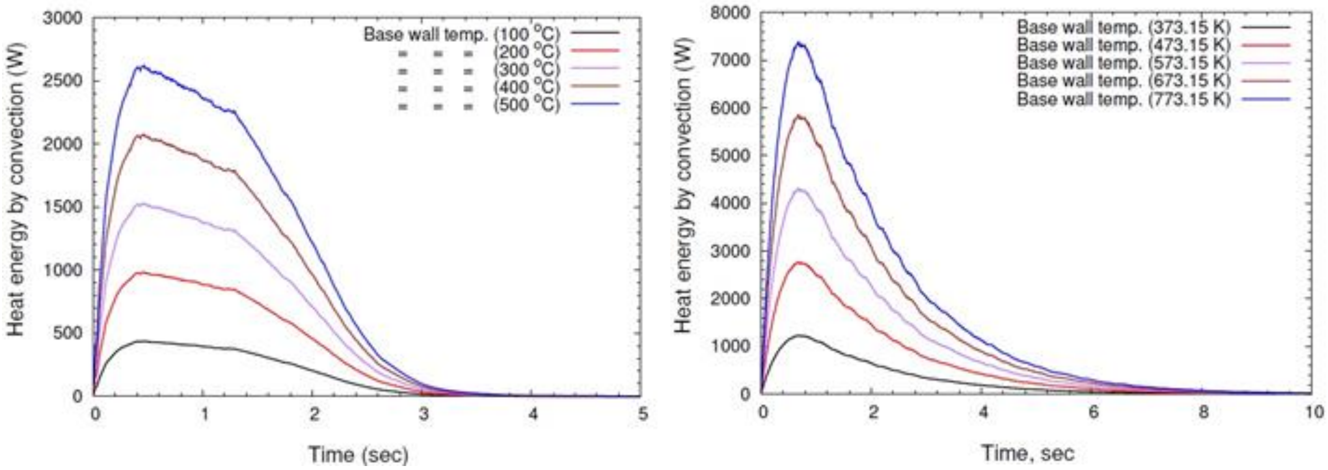

(a) **(b)**

Figure 13: Illustration of the temporal development of convective heat transfer in fluidized beds of (a) aluminum (Al) particles and (b) chromium oxide (Cr_2O_3) particles. The computations were performed at an inlet fluid velocity of 0.12 m/s. The differences in heat transfer characteristics based on the properties of the particles are emphasized in the figure, illustrating the development of the convective process with time.

At the highest inlet fluid velocity of 0.16 m/s (Fig. 14), the bed is strongly fluidized, and convection is dominant in heat transfer. In such a case, the chromium oxide particles experience more than 9000 W convective heat transfer (Fig. 14b), which is more than four times that of aluminum (Fig. 14a). This large enhancement is primarily due to the higher density of chromium oxide (5210 kg/m³), which makes the particles more inertial and thus more strongly coupled with fluid drag. As the velocity increases, the drag forces increase, leading to stronger particle circulation and mixing, which in turn continuously enhances the convective heat transfer by renewing the thermal boundary layer.

Although aluminum has higher thermal conductivity, it is observed from the results that, at higher velocities, hydrodynamic forces (inertia, slip, and momentum transfer) play a more significant role than conductivity. Hence, chromium oxide exhibits better convective heat transfer due to the dominant role of fluid-solid dynamic interactions in heat transport during fluidization.

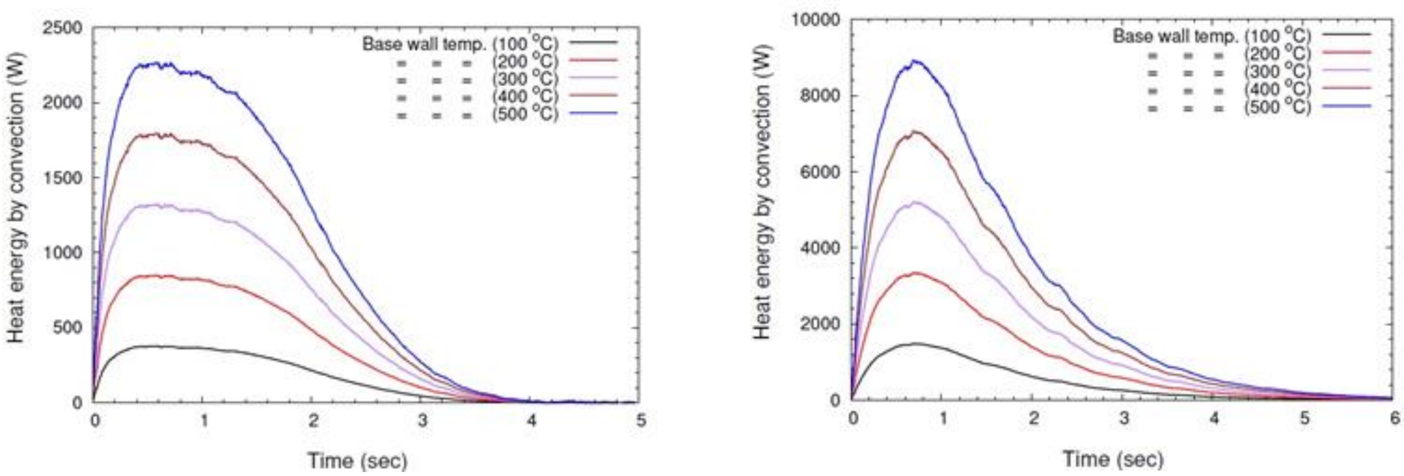

(a) **(b)**

Figure 14: Illustration of the temporal development of convective heat transfer in fluidized beds of (a) aluminum (Al) particles and (b) chromium oxide (Cr_2O_3) particles. The computations were performed at an inlet fluid velocity of 0.16 m/s. The differences in heat transfer characteristics based on the properties of the particles are emphasized in the figure, illustrating the development of the convective process with time.

The radiation heat transfer in the fluid-solid packed and fluidized beds is normally less than the conduction and convection heat transfers due to the relatively small size of the particles. However, when the wall temperature is high, the radiation heat transfer becomes more significant because the radiation heat transfer is strongly dependent on temperature ($\propto T^4$). Thus, even a small rise in wall temperature can significantly enhance the radiation heat transfer.

In Fig. 15, at the lower fluid velocity (v_f = 0.08 m/s), the bed is in the dense packed-like state, which means that the particles are packed in a close manner and their movement is restricted. The CFD-DEM results indicate that the radiation heat energy of chromium oxide particles is about 0.024 W at 500°C after 14 seconds (Fig. 15b), whereas the aluminum particles are only about 0.0045 W (Fig. 15a). The huge difference between the two is primarily due to the difference in the emissivity of the materials (Table 2). Chromium oxide has a much higher emissivity, which means that it can better absorb and emit thermal radiation, resulting in a higher rate of radiative heat transfer. Aluminum, on the other hand, has a lower emissivity and acts more like a reflective surface, making it less capable of taking part in a radiation process. Thus, the above trend clearly verifies that in a dense bed with high wall temperature, radiation becomes material-dependent, and the emissivity of the particulate phase is the primary controlling factor, even if the hydrodynamic conditions are kept unchanged.

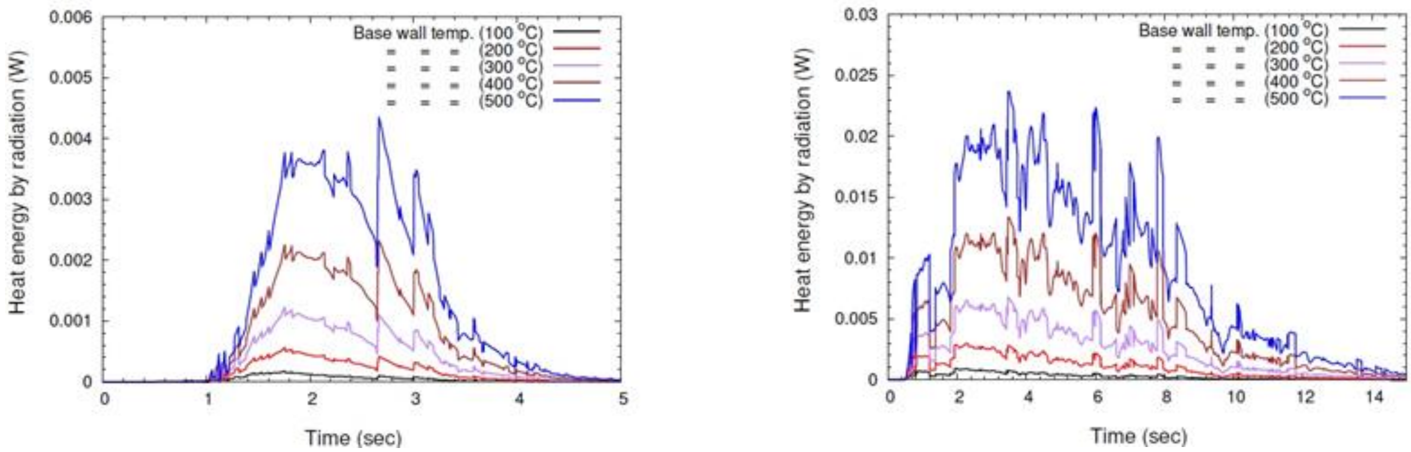

(a) (b)

Figure 15: Illustration of the temporal variation of radiative heat transfer in fluidized beds of (a) aluminum (Al) particles and (b) chromium oxide (Cr_2O_3) particles at a superficial fluid velocity of 0.08 m/s. This graph indicates the change in the value of radiative heat transfer with time, taking into account the differences in the radiative properties of the particles.

With increasing inlet fluid velocity (v_f = 0.12-0.16 m/s), Figs. (16 and 17), The contribution of chromium oxide particles to radiative heat transfer rises continuously to a maximum of 0.039 W (Fig. 17 b). This trend is largely linked to the changes in the structure of the bed due to the rising hydrodynamic forces. At higher fluid velocities, the bed becomes more expanded and dynamic, resulting in higher particle separation and lower particle clustering. Consequently, a higher proportion of the particle surface area is directly exposed to the surrounding surfaces and environment, as opposed to being shielded by other particles. This shielding or shading effect is a major factor that reduces the effective radiating area, thus increasing the amount of thermal radiation that can be emitted.

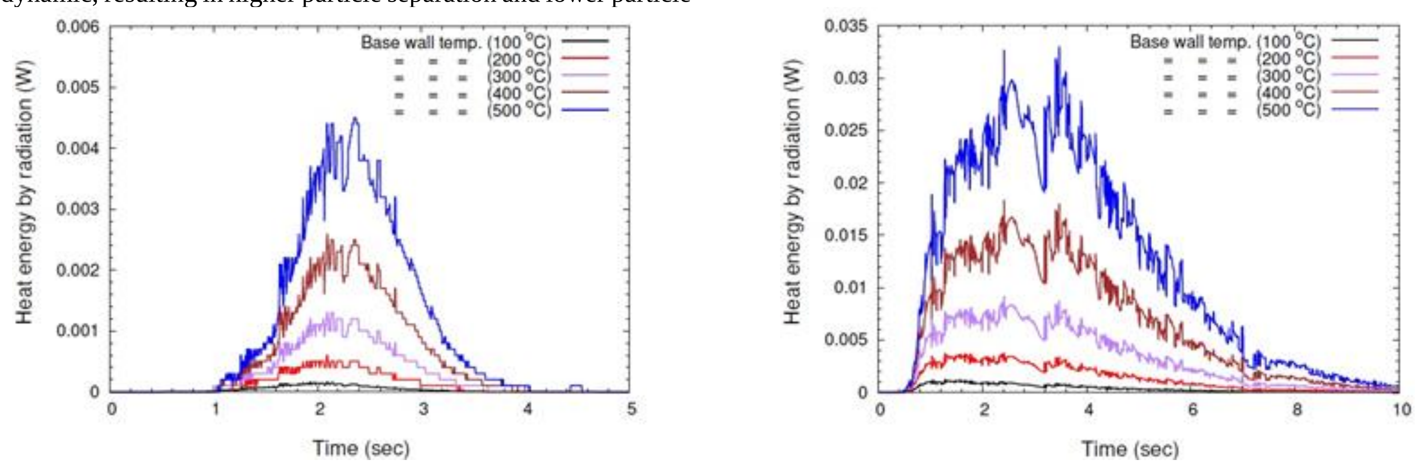

(a) (b)

Figure 16: Illustration of the temporal variation of radiative heat transfer in fluidized beds of (a) aluminum (Al) particles and (b) chromium oxide (Cr_2O_3) particles at a superficial fluid velocity of 0.12 m/s. This graph indicates the change in the value of radiative heat transfer with time, taking into account the differences in the radiative properties of the particles.

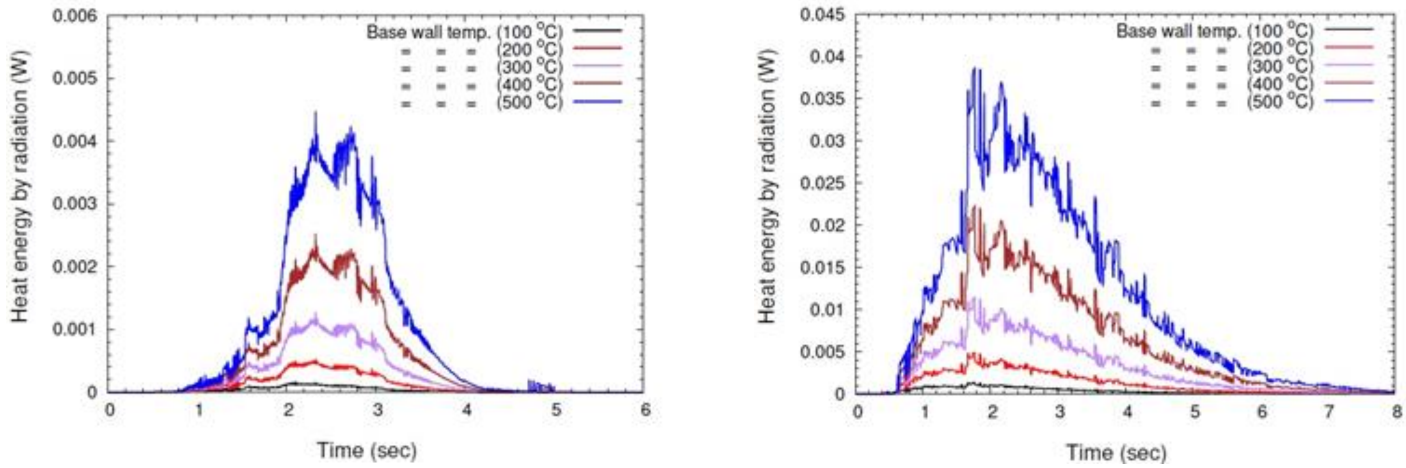

(a) (b)

Figure 17: Illustration of the temporal variation of radiative heat transfer in fluidized beds of (a) aluminum (Al) particles and (b) chromium oxide (Cr_2O_3) particles at a superficial fluid velocity of 0.16 m/s. This graph indicates the change in the value of radiative heat transfer with time, taking into account the differences in the radiative properties of the particles.

These numerical findings validate that radiation is a non-negligible heat transfer mode at high wall temperatures for beds with high emissivity materials. Hence, both material and structural design must be taken into account in the thermal design of fluidized systems to take advantage of or counteract radiation heat transfer influences, particularly at high temperatures. The numerical results of heat transfer in fluidized beds showed consistency with the experimental data in the literature [65-67].

6. 6 Particle-Fluid Heat Transfer Coefficient (Al vs. Cr_2O_3)

To gain insight into the effect of particle material on the thermal characteristics of the bed, the particle-fluid heat transfer coefficient was calculated for aluminum (Al) and chromium oxide (Cr_2O_3) particles under the same operating conditions to understand the effect of particle material on convective heat transfer. The heat transfer coefficient was calculated from the CFD-DEM thermal coupling model based on convective heat transfer between the fluid and solid phases.

Analysis of the results reveals that there are significant differences between Al and Cr_2O_3 because of their different thermo-physical properties. The Al particles respond faster to the temperature changes due to their higher thermal conductivity, and hence, there is a more uniform distribution of temperature in the particles. The Cr_2O_3 particles take longer to release heat, and hence, there is a higher temperature gradient and a lower rate of temperature change.

The findings show that the heat transfer in the fluidized bed is dominated by the convection process because of the constant mixing of particles, which leads to the renewal of the surrounding fluid and minimizes the thermal boundary layer resistance. With the increase in the inlet velocity, the convective heat transfer process is intensified, and the conductive heat transfer process is reduced because of the expansion of the bed, which leads to a decrease in particle interactions and contact time. The smaller particles result in higher heat transfer rates because of their higher surface area-to-volume ratio and better fluid-solid interaction. Moreover, the larger columns minimize the wall effects and lead to better circulation, resulting in a uniform temperature distribution and higher heat transfer rates. Compared to the fluidized bed, the packed bed has a slower heat transfer rate because of the stationary particles, which are in contact for a shorter duration, leading to the dominance of the conduction process. The role of material properties is also significant, in which aluminum particles exhibit a faster heating/cooling rate than Cr_2O_3 due to their higher thermal conductivity. The effect of radiation is negligible under the considered conditions because of the moderate temperature range and shielding of particles. Finally, the agreement between the CFD-DEM simulation results and the experimental trends validates the accuracy of the model in predicting the hydrodynamic and thermal phenomena.

7 Conclusion

In the present work, a complete CFD–DEM model was formulated and used to quantify the role of conduction, convection, and radiation heat transfer mechanisms in fluid-solid packed and fluidized beds. The numerical results were successfully compared with existing experimental results, and the agreement was satisfactory, indicating the ability of the CFD-DEM model to accurately simulate both hydrodynamic and thermal phenomena. This comparison is an indication of the accuracy of the thermal model used in this study and can be employed as a predictive model for multiphase thermal systems.

A parametric study was performed over a broad range of temperatures (100-500 °C) and for three superficial inlet velocities (0.08, 0.12, and 0.16 m/s) to cover both packed and fluidized beds. The results clearly indicated that the main heat transfer mechanism is highly dependent on both flow conditions and particle properties. In the packed bed regime, the main heat transfer mechanism was conduction, especially at the lowest velocity (0.08 m/s), where the motion of particles was restricted. Under such conditions, aluminum particles were found to be the best conductors because of their high thermal conductivity. Conversely, the augmentation of inlet velocity promoted particle-fluid interactions and mixing, resulting in a significant increase in convective heat transfer, particularly in the fluidized region. At 0.16 m/s, convection emerged as the principal heat transfer process, with aluminum particles registering higher overall heat transfer rates owing to enhanced interphase heat transfer.

Moreover, the results revealed that radiation heat transfer was insignificant in low and medium temperature conditions but significantly increased in high-temperature conditions (above 400 °C). The chromium oxide particles exhibited a higher level of radiative heat transfer owing to their higher emissivity, with radiation effects becoming more significant in the upper bed region where higher temperature gradients existed. Overall, the results clearly establish that aluminum particles are more effective in promoting conduction and convection, while chromium oxide particles are more effective in high-temperature radiation.

The findings of the present study offer significant mechanistic understanding and practical guidance on heat transfer enhancement in packed and fluidized beds and can be used to optimize thermal performance in industrial equipment such as fluidized bed reactors, dryers, and multiphase heat exchangers. Notably, the CFD-DEM approach showed significant potential in capturing granular thermal interactions and simulating heat transfer in different regimes with high accuracy.

Future studies should focus on polydisperse and non-spherical particles, temperature-dependent properties, and more complex thermal boundary conditions. Experimental verification at high temperatures and the incorporation of other physical phenomena, such as phase change and reactive heat transfer, would help to enhance the model's relevance to industrial-scale thermal processing systems.

8 Authors' contribution statement

This research was fully conceived, structured, and carried out by the author. All components of the study, such as conceptualization, design, supervision, project administration, methodology, and supervision, writing, analysis, original draft preparation, proofreading, and the preparation of the manuscript, were completed independently, guaranteeing a thorough and impartial investigation of the topic.

9 Ethical statement

In fact, this research did not need human participants or personal data, and thus ethical clearance and consent from human participants/animal subjects were not necessary.

10 Availability of data and material

Data will be made available on request.

11 Funding

There is no funding for the publication of this research paper.

12 Conflict of interest

The author of this research states that they have no conflicts of interest with regard to its publication.

13 AI Usage Declaration

The author wishes to confirm that he did not use generative AI tools during the preparation of this manuscript.

14 References

[1] Omori, Y. *Blast Furnace Phenomena and Modeling*. (London: Elsevier Applied Science, 1987).

[2] Dong, XF, Yu, AB, Yagi, JI, Zulli, P. Modelling of multiphase flow in a blast furnace: Recent developments and future work, Iron and Steel Institute of Japan International **47**, 1553-1570, doi: 10.2355/isijinternational.47.1553 (2007).

[3] Osnes, AN, Vartdal, M. Performance of drag force models for shock-accelerated flow in dense particle suspensions. International Journal Multiphase Flow **137**,103563, doi: 10.1016/j.ijmultiphaseflow.2021.103563 (2021).

[4] Vahid, T, Alberto, P, Shankar, S. Particle-resolved simulation of freely evolving particle suspensions: Flow physics and modeling. International Journal Multiphase Flow **135**, 103533, doi: 10.1016/j.ijmultiphaseflow.2020.103533 (2020).

[5] Adapa, RS, Zhang, X, Feng, T, Man Chung, K, Albrecht, JK, Ho, KC, Madden, AD, Chen, R. Heat transfer coefficients of moving particle beds from flow-dependent thermal conductivity and near-wall resistance. Solar Energy **282**, 112960, doi: 10.1016/j.solener.2024.112960 (2024).

[6] Dittus, FW, Boelter, LMK. Heat Transfer in Automobile Radiators of the Tubular Type, University of California Press, Berkeley, University of California Publications in Engineering **2**, 443-461 (1930).

[7] Zehner, P, Bauer, G, Schlünder, EU. Einfluß der Wärmestrahlung auf den Wärmeübergang in durchströmten Kugelschüttungen, Chemie Ingenieur Technik **30** (9), 433-441 (1958).

[8] Kunii, D, Smith JM. Heat Transfer Characteristics of Porous Rocks. AIChE Journal **6**, 71-78, doi: 10.1002/aic.690060115 (1960).

[9] Gunn, D J. Transfer of heat or mass to particles in fixed and fluidized beds, International Journal Heat Mass Transfer **21**(4), 467-476, doi: 10.1016/0017-9310(78)90080-7 (1978).

[10] Kunii, D, Levenspiel, O. *Fluidization Engineering*. (2nd ed., Butterworth-Heinemann, 1991).

[11] Kolar, KA, Sastri, VMK. Extended surface heat transfer in fluidized beds. Chemical Engineering Process. : Intensification **22**(1), 1-17, doi: 10.1016/0255-2701(87)80024-7 (1987).

[12] Saxena, SC, Vadivelan, K. Heat transfer in fluidized beds: Review and analysis, Chemical Engineering Communication **75**(1), 1-44 (1988).

[13] Wakao, N, Kaguei, S. *Heat and mass transfer in packed beds*. (New York, Gordon and Breach Science Publishers, 1982).

[14] Molerus, O, Wirth, K E. *Heat transfer in fluidized beds*. (London: Chapman and Hall, 1997).

[15] Botterill, JSM. *Fluid-bed heat transfer*. (New York, Academic Press, London, 1975).
[16] Martin, H. Fluid bed heat exchangers: A new model for particle convective energy transfer. Chemical Engineering Communication **13** (1-3), 1-16, doi: 10.1080/00986448108910891 (1981).
[17] Decker, N, Glicksman, LR. Heat transfer in large particle fluidized beds. International Journal Heat Mass Transfer **26** (9), 1307-1320, doi: 10.1016/S0017-9310(83)80062-3 (1983).
[18] Phillips, MC. A parametric sensitivity study on the relative importance of packet formation and single-particle motion in fluidized bed heat transfer. Chemical Engineering Science **45** (8), 2195-2202, doi: 10.1016/0009-2509(90)80095-V (1990).
[19] Agarwal, PK. Transport phenomena in multi-particle systems-IV. Heat transfer to a large freely moving particle in a gas fluidized bed of smaller particles. Chemical Engineering Science **46**, 1115-1127, doi: 10.1016/0009-2509(91)85104-6 (1991).
[20] Molerus, O, Burshka, A, Dietz, S. Particle migration at solid surface and heat transfer in bubbling fluidized beds -I. Particle migration measurement system. Chemical Engineering Science **50** (5), 871-877, doi: 10.1016/0009-2509(94)00446-X (1995).
[21] Parmar, MS, Hayhurst, AN. The heat transfer coefficient for a freely moving sphere in a bubbling fluidised bed. Chemical Engineering Science **57**, 3485-3494, doi: 10.1016/S0009-2509(02)00259-2 (2002).
[22] Collier, AP, Hayhurst, AN, Richardson, JL, Scott, SA. The heat transfer coefficient between a particle and a bed (packed or fluidised) of much larger particles. Chemical Engineering Science **59** (46), 13-4620, doi: 10.1016/j.ces.2004.07.029 (2004).
[23] Patil, AV, Peters, E, Sutkar, VS, Deen, NG, Kuipers, JAM. A study of heat transfer in fluidized beds using an integrated DIA/PIV/IR technique. Chemical Engineering Science **259**, 90-106, doi: 10.1016/j.cej.2014.07.107 (2015).
[24] Scott, SA, Davidson, JF, Dennis, JS, Hayhurst, AN. Heat transfer to a single sphere immersed in beds of particles supplied by gas at rates above and below minimum fluidization. *Industrial & Engineering Chemistry Research* **43**, 5632-5644, doi: 10.1021/ie0307380 (2004).
[25] Di Natale, F, Lancia, A, Nigro, R. A single particle model for surface-to-bed heat transfer in fluidized beds. Powder Technology **87**, 68-78, doi: 10.1016/j.powtec.2008.01.014 (2008).
[26] Zhou, ZY, Yu, AB. Particle Scale Study of Heat Transfer in Packed and Bubbling Fluidized Beds. AIChE Journal **55** (4), 868-884, doi: 10.1002/aic.11823 (2009).
[27] Cundall, PA, Strack, ODL. A discrete numerical model for granular assemblies. Geotechnique **29**, 47-65, doi: 10.1680/geot.1979.29.1.47 (1979).
[28] Archambeau, K, Méchitoua, N, Sakiz, M. Code Saturne: A Finite Volume Code for the computation of turbulent incompressible flows - Industrial Applications, International Journal on Finite Volumes **1**(1), 1-62, http://www.latp.univ-mrs.fr/IJFV/spip.php?article3 (2004).
[29] Tsuji, Y, Kawaguchi, T, Tanaka, T. Discrete particle simulation of two-dimensional fluidized bed. Powder Technology **77**(1), 79-87, doi: 10.1016/0032-5910(93)85010-7 (1993).
[30] Xu, BH, Yu, AB. Numerical simulation of the gas-solid flow in a fluidized bed by combining the discrete particle method with computational fluid dynamics. Chemical Engineering Science **52**(16), 2785-2809, doi: 10.1016/S0009-2509(97)00081-X (1997).
[31] Subburaj, R, Tang, Y, Deen, NG. Euler-Lagrange Simulations of Microstructured Bubble Columns Using a Novel Cutting Model. *Industrial & Engineering Chemistry Research* **62** (38), 15656-15665, DOI: 10.1021/acs.iecr.3c02352 (2023).
[32] Lu, B, Third, JR, Müller, CR. Heat transfer in packed beds: A DEM study. AIChE Journal **55**(11), 2866-2875, (2009).
[33] Adapa, RS, Zhang, X, Feng, T, Man Chung, K, Albrecht, JK, Ho, KC, Madden, AD, Chen, R. Heat transfer coefficients of moving particle beds from flow-dependent thermal conductivity and near-wall resistance. Solar Energy **282**, 112960, doi: 10.1016/j.solener.2024.112960 (2024).
[34] de Munck, MJA, Peters, EAJF, Kuipers, JAM. CFD-DEM modeling and validation of solids drying in a gas-fluidized bed. Chemical Engineering Science, **291**, 119922, doi: 10.1016/j.ces.2024.119922 (2024).
[35] de Munck, MJA, Boersma, BJ, van der Hoef, MA, Kuipers, JAM. Coarse-grained CFD-DEM modeling of heat transfer in fluidized beds. Chemical Engineering Science **280**, 5 119048. doi: 10.1016/j.ces.2023.119048 (2023).
[36] Zhou, Q, Zhang, J, Yang, N. CFD-DEM simulation of particle-fluid heat transfer in bubbling fluidized beds. Powder Technology **203**(2), 435-44, doi: 10.1016/j.powtec.2010.03.073 (2010).
[37] Zhang, Q, Xia, Y, Cheng, Z, Quan, X. DEM-CFD Simulation Analysis of Heat Transfer Characteristics for Hydrogen Flow in Randomly Packed Beds. Energies **17** (9), 2226, doi: 10.3390/en 17092226 (2024).
[38] Quan, X, Xia, Y, Zhang, Q. CFD-DEM Modeling of Cryogenic Hydrogen Flow and Heat Transfer in Packed Bed. Sustainability **16** (11), 4522, doi: 10.3390/su 16114522 (2024).
[39] Tsory, T, Ben-Jacob, N, Brosh, T, Levy, A.Thermal DEM-CFD modeling of packed bed heat transfer, Powder Technology **244**, 52-60, doi: 10.1016/j.powtec.2013.04.013 (2013).
[40] Wu, H, Gui, N, Yang, X, Tu, J, Jiang, S. Parameter analysis and wall effect of radiative heat transfer for CFD-DEM simulation in nuclear packed pebble bed. *Experimental and Computational Multiphase Flow* **3**(4), 250-257, doi.org/10.1007/s42757-020-0058-2 (2021).
[41] Baniasadi, M, Peters, B. Coupled CFD-DEM with heat and mass transfer to investigate the melting of a granular packed bed. Chemical Engineering Science **178**, 136-145, doi: 10.1016/j.ces.2017.12.044 (2018).
[42] Wu, H, Gui, N, Yang, X, Tu, J, Jiang, S. Numerical simulation of heat transfer in packed pebble beds with thermal radiation, International Journal of Heat and Mass Transfer **110**, 393-405, doi: 10.1016/j.ijheatmasstransfer.2017.03.035(2017).
[43] Wang, S, Luo, K, Hu, C, Lin, J, Fan, J. CFD-DEM simulation of heat transfer in fluidized beds: verification and application. Chemical Engineering Science **197** (6), 280-295, doi: 10.1016/j.ces.2018.12.031 (2019).
[44] Jun, X, Miaomiao, N. CFD-DEM simulation of heat transfer during the biomass combustion process in fluidized beds. Mechanics in Engineering **44** (4), 844-851, doi: 10.6052/1000-0879-22-197 (2022).
[45] Hoorijani, H, Esgandari, B, Zarghami, R, Sotudeh-Gharebagh, R, Mostoufi, N. CFD-DEM modeling of heat transfer in a spouted pulsed fluidized bed. Industrial & Engineering Chemistry Research **200**, 95-106, doi: 10.1016/j.cherd.2023.10.030 (2023).

[46] Hu, Y, Chen, L, Liu, Z, Ma, H, Zhou, L, Zhao, Y. CFD-DEM Modeling and Experimental Verification of Heat Transfer Behaviors of Cylindrical Biomass Particles with Super-Ellipsoid Model. Energies **18**(6),1504, doi: 10.3390/en18061504 (2025).

[47] Gan, J, Zhou, Z, Yu, A. Particle scale study of heat transfer in packed and fluidized beds of ellipsoidal particles. Chemical Engineering Science **144**, 201-215, doi: 10.1016/j.ces.2016.01.041(2016).

[48] Bellan, S, Matsubara, K, Cho, HS, Gokon, N, Kodama, T. A CFD-DEM study of hydrodynamics with heat transfer in a gas-solid fluidized bed reactor for solar thermal applications. International Journal of Heat and Mass Transfer **116**, 377392, (2018).

[49] Qiu, K, Wu, F, Yang, S, Luo, K, Luo, KK, Fan, J. Heat transfer and erosion mechanisms of an immersed tube in a bubbling fluidized bed: a LES-DEM approach. International Journal of Thermal Science **100**, 357-371, doi: 10.1016/j.ijthermalsci.2015.10.001 (2016).

[50] Al-Arkawazi, S, Marie, C, Coorevits, P. Modeling the heat transfer between fluid and granular medium. Applied Thermal Engineering **128**, 696-705, doi: 10.1016/j.applthermaleng.2017.09.064 (2018).

[51] Flamarz, SA. Computational Study of Heat Transfer Behavior in Fluid-Solid Fluidized Beds. Sulaimani Journal for Engineering Science **7** (3), 35-45, doi: 10.17656/sjes.10132 (2020).

[52] Brosh, T, Levy, A. Modeling of heat transfer in pneumatic conveyer using a combined DEM-CFD numerical code. Drying Technology **28**, 155-164, doi: 10.1080/07373930903517482 (2010).

[53] Brosh, T, Kalman, H, Levy, A. DEM simulation of particle attrition in dilute-phase pneumatic conveying. Granular Matter **2**, 175-181, doi: 10.1007/s10035-010-0201-z (2010).

[54] Fortin, J, De Saxcé, G. Modélisation numérique des milieux granulaires par l'approche du bi-potentiel. Comptes Rendus de l'Académie des Sciences - Series IIB - Mechanics-Physics-Astronomy **327**, 721-724, doi: 10.1016/S1287-4620(99)80126-4 (1999).

[55] Fortin, J, Coorevits, P. Selecting contact particles in dynamic granular mechanics systems. Journal Computer Applied Mathematics **168**, 207–213, doi.org/10.1016/j.cam.2003.05.025 (2004).

[56] Al-Arkawazi, S. Modélisation des interactions fluide-milieu granulaire par couplage CFD-DEM, incluant les transferts thermiques. (PhD Thesis, Sciences, Technologies et Santé. Université de Picardie Jules Verne, 2014).

[57] Al-Arkawazi, S. Evaluate the Effect of Drag Force Models on the Fluidization Process. Passer **7** (2), 1053-1063, DOI: 10.24271/PSR.2025.535255.2264 (2025).

[58] Di Felice, R. The voidage function for fluid-particle interaction systems. International Journal Multiphase Flow **20** (1), 153-159, doi: 10.1016/0301-9322(94)90011-6 (1994).

[59] Mindlin, RD, Deresiewicz, H. Elastic Spheres in Contact under Varying Oblique Forces. Journal Applied Mechanics **20**, 327-344, (1953).

[60] Zabrodsky, SS. *Hydrodynamics and Heat Transfer in Fluidized Beds*, (M.I.T Press, Cambridge, Massachusetts,1966).

[61] Laguerre, O, Amara, SB, Flick, D. Heat transfer between wall and packed bed crossed by low velocity airflow. Applied Thermal Engineering. 2006; **26** (16): 1951-1960. doi: 10.1016/j.applthermaleng.2006.01.011.

[62] Messai, S, El Ganaoui, M, Sghaier, J, Belghith, A. Experimental study of the convective heat transfer coefficient in a packed bed at low Reynolds numbers. Thermal Science Journal. 2014; **18** (2), 443-450. doi: 10.2298/TSCI120715108M.

[63] Wen, DT, Cong, TN, He, Y, Chen, H, Ding, Y. Heat transfer of gas-solid two-phase mixtures flowing through a packed bed. Chemical Engineering Science **62**, 4241-4249, doi: 10.1016/j.cej.2006.11.006 (2007).

[64] L. M. Ferreira, J. A. M. Castro, and A. E. Rodrigues, An analytic and experimental study of heat transfer in fixed bed. International Journal of Heat and Mass Transfer **45**, 951-961, doi: 10.1016/S0017-9310(01)00209-5 (2002).

[65] Gunn, DJ, Hilal, N. Heat transfer from vertical surfaces to dense gas-fluidized beds. International Journal of Heat and Mass Transfer **37** (16), 2465-2473, doi.org/10.1016/0017-9310(94)90286-0 (1994).

[66] Lee, JC, Han, GY, Yi, CK. Heat transfer in a high temperature fluidized beds. Korean Journal of Chemical Engineering **16** (20), 260-264, doi: 10.1007/BF02706846 (1999).

[67] Stenberg, V, Sköldberg, V, Öhrby, L, Rydén, M. Evaluation of bed-to-tube surface heat transfer coefficient for a horizontal tube in bubbling fluidized bed at high temperature. Powder Technology **352**, 488-500, doi: 10.1016/j.powtec.2019.04.073 (2019).